

# Soil system dynamics for learning about complex, feedback-driven agricultural resource problems: model development, evaluation, and sensitivity analysis of biophysical feedbacks

Benjamin L. Turner<sup>a,\*</sup>, Srinadh Kodali<sup>b</sup>

<sup>a</sup> Assistant Professor, Department of Agriculture, Agribusiness, and Environmental Science and King Ranch® Institute for Ranch Management, Texas A&M University-Kingsville, 700 University Blvd., MSC 228, Kingsville, TX 78363

<sup>b</sup> Graduate Research Assistant, Department of Agriculture, Agribusiness, and Environmental Science, Texas A&M University-Kingsville, 700 University Blvd., MSC 228, Kingsville, TX 78363

## ARTICLE INFO

### Keywords:

Soil moisture  
Irrigation  
Fertilization  
Soil salinity  
Agroecosystems  
System dynamics

## ABSTRACT

Soils form the foundation of terrestrial ecosystems that regulate the processes and functions driving ecosystem goods and services provisions that humans rely on, including agriculture. Pressing agricultural resource challenges persist, including those involving irrigation, fertilization, and salinization, due to the complex, coupled, and feedback-driven connectivity of various soil processes that are difficult to manage. Soil moisture dynamics cross-cut these processes and is a logical integration point for generating understanding and new insights for improved agroecosystem management. This paper presents an integrated soil-water-nutrient-plant interaction model (built within a system dynamics framework) with the purpose of replicating soil moisture evolution for a set of unique soils and climates, examining model performance given common irrigation (e.g., frequency and application rates) and crop management considerations (e.g., fertilization, tillage, cover cropping), and evaluating via sensitivity analysis model robustness and quantifying influential management parameters effect on core bio-physical feedbacks at the soil-level. The model has four main state variables (soil moisture, soil nitrogen, soil sodium, and plant canopy cover) that interact dynamically via feedback processes (formulated as coupled partial differential equations) between them. Exogenous variables included precipitation time-series data and required climatic parameters to determine reference (potential) evapotranspiration. The time-unit used from simulation was 1 day (time-step = 0.25) with a simulation horizon of 365 days. The model was calibrated using a variety of sources in the literature and with comparison to observed soil moisture data from four sites in Texas, USA, and evaluated statistically for accuracy (mean bias), precision, (coefficient of determination), and overall fit (Theil inequality statistics). Sensitivity analyses were conducted for a variety of hydroclimate forcing and irrigation, fertilization, and crop management decisions to examine the impacts to soil moisture evolution, soil salinity, and cropping profitability, among other variables. Calibration results showed high degrees of agreement between observed and predicted values (mean  $r^2 = 0.67$ , mean bias = 0.008%). Sensitivity results demonstrated that precipitation frequency was more influential than precipitation depth in regulating soil moisture, that irrigation threshold (i.e., the soil moisture level inducing irrigation) was the variable most influential to crop profitability (which was maximized at the lowest irrigation threshold value), and that several conservation management strategies (i.e., no-till with residue management or cover cropping) improved soil moisture and crop profitability, contrary to common management perceptions. Several other tests for alternative fertilization, irrigation, and tile drain installation strategies produced results that corroborate common observations of agroecosystem management (i.e., despite environmental risks, crop profitability was enhanced). Future model extensions include expansion of the irrigation, fertilization, and crop management decision making factors to better capture how decisions that respond to economic and policy signals influence resource use and soil system dynamics. Modeling these complex, feedback driven agroecosystems processes remains an arena for future modeling innovations that will support important resource management improvements.

\* Corresponding author.

E-mail addresses: [benjamin.turner@tamuk.edu](mailto:benjamin.turner@tamuk.edu) (B.L. Turner), [srinadh.kodali@students.tamuk.edu](mailto:srinadh.kodali@students.tamuk.edu) (S. Kodali).

## 1. Introduction

Soils are the foundation of terrestrial ecosystems, and as such, functioning soil systems are critical to the sustainability of ecosystem processes, particularly nutrient cycling of carbon, nitrogen, and water (Adhikari and Hartemink, 2016, Swift et al., 2004) that provide wide ranging ecosystem goods and services for human well-being (Adhikari and Hartemink, 2016), including agricultural production (Power, 2010). Humans rely on these processes for the regulation and provisioning of food production as well as fresh water. The sustainability of these functions are currently at risk due to agricultural intensification and expansion of cultivated landscapes, both considered vital strategies to meet rising food, feed, and bioenergy demand induced by global population growth (Alexander et al., 2015, Power, 2010, Turner et al., 2018a). Unfortunately, both cultivation expansion (extensification) and intensification (increased factor productivity on existing agricultural lands) have created a number of unintended consequences that may weaken efforts to achieve global food security, including (but not limited to): groundwater depletion, water quality contamination, increased greenhouse gas emissions, loss of soil organic carbon, soil erosion by both wind and water, and soil salinization (Turner et al., 2018a; Turner et al., 2018b; Horrigan et al., 2002; Hurni et al., 2015).

These factors and others (e.g., irrigation, fertilization and leaching) may be collectively called 21st-century challenges for agriculture due to the complex, coupled, feedback-driven connectivity that arise in attempts to meet growing societal demands (Figure 1).

For example, increased groundwater pumping for irrigation reduces water table levels, which may inadvertently raise groundwater salinity

levels and exacerbate soil salinity problems with continued irrigation applications (Gates et al., 2002, Konikow, 2013, Konikow and Kendy, 2005, Konikow and Person, 1985, Smedema and Shiati, 2002, Texas Water Development Board, 2019 United States Department of Agriculture 2014). A typical response to this problem is to “flush” the salts out by still additional water applications. Agricultural intensification via crop selection for maximum yields can also lead to heavy (or over) fertilization of nutrients (which are subject to leaching into water supplies and reduces soil microbial activity needed to sustain organic carbon levels (Carpenter et al., 1998, Matson et al., 1997, Scanlon et al., 2007, Tilman et al., 2002, International Fertilizer Association 2019), become reliant on chemical treatments to limit pest damages (which accelerates pest genetic selection for chemical resistance (Denholm, 1998, Kranthi et al., 2002, Pimentel et al., 1992, International Fertilizer Association 2012, Tilman et al., 2002), and conventional tillage (which exposes the soil surface and accelerates erosion; (Turner et al., 2018a, 2018b, Montgomery, 2007, Nearing et al., 2017, Nearing et al., 2005). Twenty-first century agricultural resource problems are therefore fundamentally coupled soil, crop and water management problems, since hydrologic processes and soil functions are not independent but are interlinked (co-dependent). This makes agricultural soil system management (defined here as management of the aboveground processes and disturbances of the soil surface down to the bottom of the rooting zone) a critical leverage point for mitigating these systemic problems.

As just indicated, typical management decisions including irrigation, fertilization, and crop and tillage decisions collectively can either strengthen or weaken the ability of a soil systems to function, such as nutrient retention, water cycling, and shallow groundwater recharge

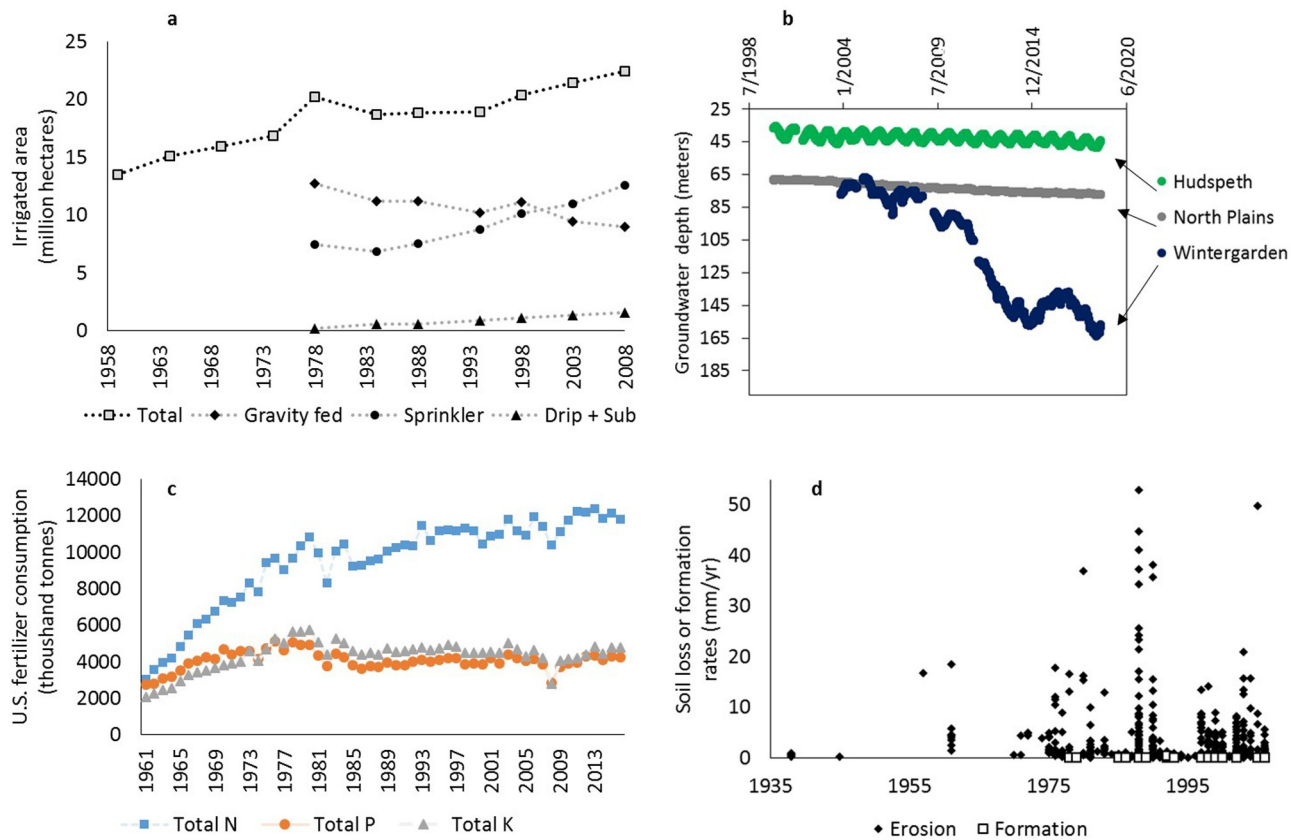


**Figure 1.** Example trends-over-time of several important agroecosystem factors representative of common 21st century resource management problems, including irrigation expansion (panel a, data from USDA Farm and Ranch Irrigation Survey (United States Department of Agriculture 2014), groundwater depletion in several arid/semi-arid agricultural regions of Texas, USA (panel b, data from Texas Water Development Board (Texas Water Development Board, 2019), increasing fertilizer use, particularly nitrogen (panel c, data from International Fertilizer Association; International Fertilizer Association 2019), and soil formation and erosion rates (panel d, data from (Montgomery, 2007).

(Adhikari and Hartemink, 2016, Turner et al., 2018a, 2018b, Fernald et al., 2010). To add to the complexity that arises between soil processes and management decisions is the extreme hydro-climate variability (both spatially and temporally) that further complicates irrigation planning and control, fertilization efficiency, and crop productivity and profitability (Daly and Porporato, 2006). The central problem of this variability stems from the unpredictability of precipitation (Droogers et al., 2000), which is expected to become more variable under projected climate change (Mendelsohn et al., 2007, Motha and Baier, 2005). Given the connectivity between soil processes and agricultural decisions, both of which are in part driven by this extreme hydro-climate variability, particularly precipitation, understanding complex resource management problems requires a means to integrate the underlying dynamics of multiple soil, hydrologic, nutrient, and human-related factors (e.g., socio-hydrology dynamics in (Fernald et al., 2012, Gunda et al., 2018, Turner et al., 2016a); or agricultural land use dynamics in (Menendez et al., 2019, Turner et al., 2016b, Turner et al., 2017a).

Soil moisture dynamics cross-cuts each of these factors and a logical integration point for several reasons. First, soil moisture dynamics provide a link between precipitation variability (and therefore irrigation demands) and plant productivity (and therefore profitability) (Abd and Ali, 2013, Ali et al., 2007, Porporato et al., 2015, Porporato et al., 2001). Soil physical properties control the intensity and duration of soil water deficit since these properties drive the soil moisture dynamics (International Fertilizer Association 2007, Porporato et al., 2001, Power, 2010, Stephenson, 1990, Swift et al., 2004), and soil water deficits in turn regulates plant physiology since plants must uptake water from the soil (Falkenmark and Rockstrom, 2006). Second, plants productivity may be reduced to levels observed under drought conditions even with acceptable precipitation due to poor soil characteristics, particularly regarding soil hydrologic functions such as soil moisture retention (Branson et al., 1970, Branson et al., 1976, Daubenmire, 1968, Harrington, 1991, Newman, 1967, Nilsen and Orcutt, 1998, Sadras and Angus, 2006, Vico and Porporato, 2013). Third, soil water stress is often the reason for poor plant nutrient uptake, particularly nitrogen, since soil moisture regulates ammonification and nitrification and this total plant nutrient uptake (Bennett et al., 1989, Brady and Weil, 1996, Larcher, 1995, Manzoni and Porporato, 2009, Nilsen and Orcutt, 1998, Wang et al., 2012). Soil moisture is therefore a key system component capable of integrating the soil system dynamics arising from soil, climate, vegetative (crop), management (irrigation and fertilization) characteristics, and the interacting feedbacks between factors, across evapotranspiration (ET) regimes (Seneviratne et al., 2010).

Understanding these complex feedbacks and the implications they have on agroecosystem management could be aided by the use of a dynamic systems approach capable of modeling coupled soil-plant-water dynamics in relatively simple and parsimonious means. The discipline of ecohydrology has provided a hydrologic foundation from which to understand observed vegetation characteristics due to the linkages and flows between climate (e.g., stochastic precipitation), soil properties (e.g., soil water holding capacity), and vegetation (through soil-moisture mediated plant transpiration (Rodriguez Iturbe et al., 1999, Rodriguez-Iturbe, 2000, Rodriguez-Iturbe et al., 2001; Porporato et al., 2002; illustrated in Figure 2).

Well documented ecohydrology models have focused on development and analysis of analytic expressions and probability density functions that describe soil moisture characteristics (e.g., Porporato et al., 2002, De Michele et al., 2008, Laio et al., 2001a, Laio et al., 2001b, Porporato et al., 2015, Porporato et al., 2001) and only more recently matching model predicted values with observed levels of soil moisture (e.g., Kumar et al., 2013, Pan et al., 2015, Turner, 2017b, Xia and Shao, 2008). Ecohydrologic models have focused on semi-arid ecosystems like rangelands or savannas because they are primarily water-controlled (i.e., rainfall dependent), have vegetation

characteristics that are reflective of historical climate regimes and soil properties, and where vegetation often exerts control on watershed balances through myriad land-atmosphere feedbacks. More recently however, ecohydrologic models have been recognized as useful frameworks for investigating agricultural soil problems such as irrigation, fertilization, and salinity dynamics due to their parsimonious representation of soil processes, ability to capture both stochastic and dynamic coupling between state variables, and given that the underlying assumptions regarding soil and plant characteristics are well matched with typical agroecosystem (Porporato et al., 2015).

The objectives of this work were to 1) utilize the foundational framework described in the ecohydrology literature to develop a dynamic plant-soil-water-nutrient model robust enough to adequately replicate the soil moisture evolution for a variety of soils and climate conditions; 2) overlay the model with common irrigation and crop management considerations, including irrigation method, timing, and application volume, fertilization times and volumes, and no-till practices with crop residue management or cover cropping; and 3) evaluate the model using a variety of sensitivity analyses to examine both model robustness and quantify which parameters are most influential to the core biophysical feedbacks included in the model. The remainder of the paper follows with a description of the development of the model and the calibration and evaluation procedures employed to verify its ability to adequately capture the high-level feedbacks operating within a coupled plant-soil-water agroecosystem. Then, several hypothesis tests are applied to the model regarding crop and irrigation decision-making across a variety of landscape and climatic conditions. Results are then provided with a discussion centered in the context of sustainability of soil and water resources and agricultural profitability given 21st century agricultural and land-use pressures. We conclude with several recommendations and outline future research directions and model applications for both sustainability research and teaching.

## 2. Materials and Methods

### 2.1. Model overview

The model represents a soil-water-nutrient-plant continuum which integrates inflows and outflows of water and nutrients through feedbacks between soil moisture,  $S$ , expressed as a percentage of field capacity, and plant productivity,  $C$ , representing the percentage of soil surface covered, with the interaction effects of nutrient balances (nitrogen and sodium) and management factors (cropping and irrigation decisions). The model has four main state variables, soil moisture, soil nitrogen, soil sodium, and canopy cover, which interact dynamically through various feedbacks between each other. Feedback mechanisms formulated as coupled partial differential equations link  $S$  and  $C$  dynamics through a variety of processes, including infiltration and interception (capturing infiltration-excess runoff dynamics), evapotranspiration rates (which drive plant production or induce plant stress), nitrogen uptake (which either reinforces plant canopy growth), nitrogen leaching (an important factor for crop management as well as environmental quality), sodium accumulation (which may reduce plant water update), and irrigation decisions (which can respond to soil moisture conditions as well as influence nitrogen or sodium dynamics). While crop biomass production (or yield) is driven by the outcomes of the system, canopy cover does interact dynamically with water and nutrient balances via its influence on interception and transpiration terms. Exogenous variables included precipitation time-series data input and required climatic parameters to determine reference (or potential) evapotranspiration, ET. The coupled soil-water-plant model (conceptualized in Figure 3) was constructed using the system dynamics (SD) modeling environment Vensim™ (Ventana Systems, Inc.; Cambridge, MA, USA). The time unit used from simulation was 1 day, with time step = 0.25 and a simulation time horizon of 365 days. The main strengths of using the SD platform was the ease with which the

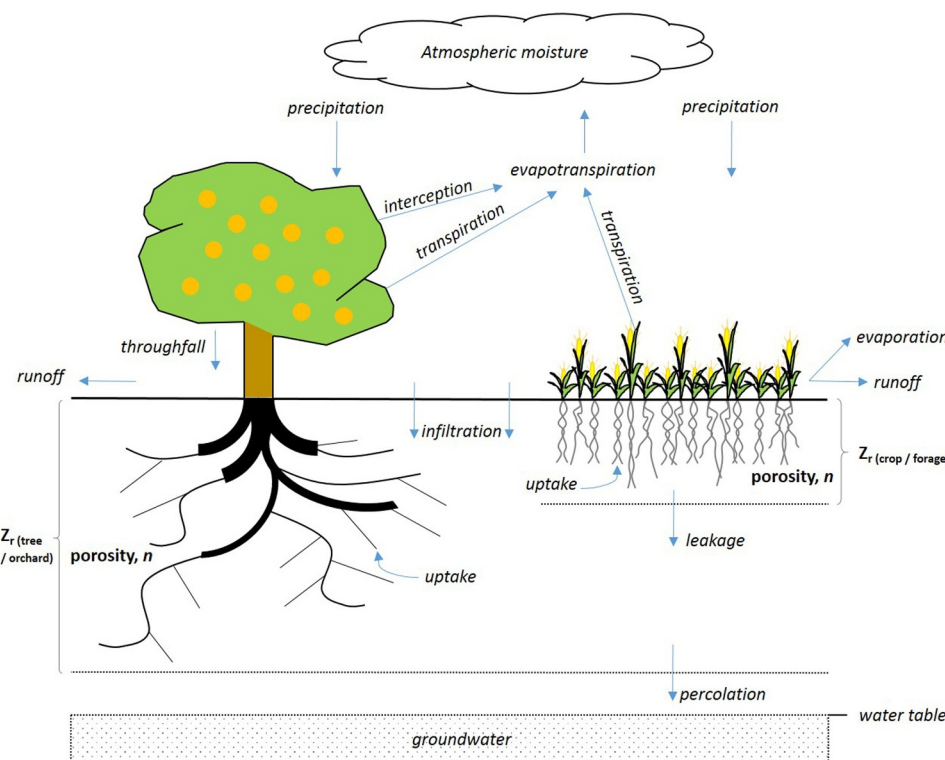


**Figure 2.** Schematic representation of critical zone water flow (indicated by the blue arrows) relevant in arid/semi-arid agroecosystems and used throughout many ecohydrologic models whose core structures incorporate soil-water balance coupled to plant productivity (through transpiration) as endogenous components driven by hydroclimate variability (primarily precipitation but also temperature).

high number of feedback mechanisms could be formalized as integrated coupled difference equations, a rapid simulation time, and a visually appealing means in which to incorporate the dynamics of interest (Turner et al., 2016c). The model was used to examine the various trajectories in soil moisture, nutrient balances, and profitability response given alternative agroecosystem features and management decisions. In the sections that follow, we describe in detail the soil-water-plant model components and their feedback connections, many aspects of which have been derived, replicated, or extended from a variety of other soil moisture, crop, or nutrient models (Kumar et al., 2013,

Laio et al., 2001a, Laio et al., 2001b, Manzoni and Porporato, 2009, Mau and Porporato, 2015, Pelak et al., 2017, Porporato et al., 2015, Porporato et al., 2001, Rodriguez-Iturbe et al., 2001, Vico and Porporato, 2011a, Vico and Porporato, 2011b, Vico and Porporato, 2013) but that have not been integrated into one cohesive model. Key model variable names and equations are provided in the sections that follow; additional descriptions of variable names, symbols, parameter values, and their sources are provided in the Appendix.

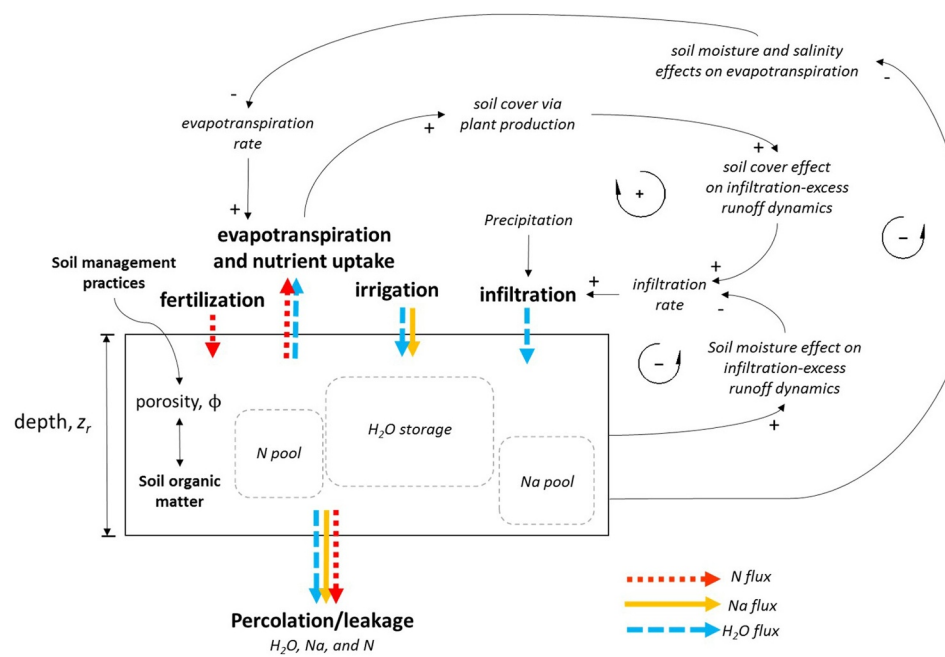


**Figure 3.** Conceptual diagram of the simplified soil profile model for a given soil depth,  $Z_r$ , of a given soil texture with nutrient fluxes acting upon the soil-water balance (thick solid and dashed arrows) on the column through infiltration, leakage or percolation, and evapotranspiration, irrigation, and fertilization (inflows represent positive links to the soil column while outflows represent negative polarity, i.e., increased outflows will reduce the nutrient level). The dynamics of the column are also influenced through several feedback mechanisms (thin black arrows) representing causal connections that drive nutrient fluxes, i.e., soil moisture effect and soil cover effect on infiltration-excess runoff dynamics (which drive infiltration rates), soil moisture and salinity effect on evapotranspiration rates (which drive plant nutrient uptake rates and therefore the other primary feedbacks). The “+” and “-“ symbols on individual links indicate link polarity between variables, signifying a positivity or negative influence, while the + and - symbols within each feedback loop denote whether the overall polarity of the feedback dynamics are positive (reinforcing) or negative (balancing/constraining) on the soil nutrient evolution.

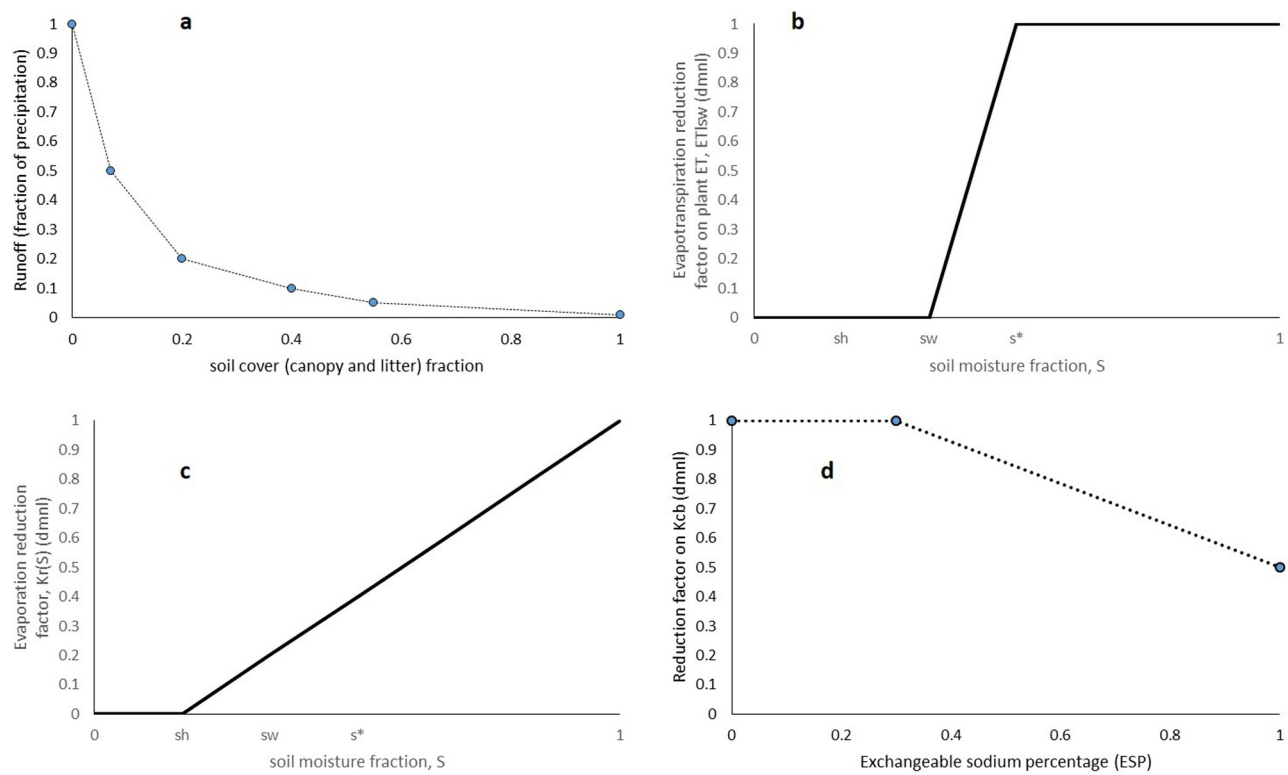


**Figure 4.** Dynamic feedback relationships between components of the model. Panel a shows the nonlinear relationship of water runoff driven by canopy cover,  $C$ ; panel b displays the behavior of the evapotranspiration reduction factor acting on ET from soil water storage as a function of percentage soil moisture of field capacity,  $S$ , where  $s_h$ ,  $s_w$ ,  $s^*$ , and  $s_{fc}$  are the soil moisture levels that induce plant-water hydroscopic stress, plant-water wilting stress, the soil moisture level that is non-limiting to ET, and soil moisture field capacity, respectively; panel c shows the linear dependence of the evaporation reduction factor on soil moisture,  $S$ ; and panel d displays the influence of exchangeable sodium percentage (ESP) on the basal crop coefficient,  $K_{cb}$ , a critical factor determining ET.

## 2.2. Soil water balance dynamics

Soil moisture was modeled as the balance between moisture gains (precipitation and irrigation) and losses (evapotranspiration and leakage), expressed as:

$$nZ_r(dS/dt) = R(t) + I(S(t)) - ET(S(t), C(t)) - Q(S(t)), \quad (1)$$

where  $n$  is the soil porosity,  $Z_r$  is the active soil rooting depth,  $S$  is the vertically averaged relative soil moisture content ( $0 \leq S \leq 1$ , where 1 is fully saturated conditions).  $R(t)$  represents the inflow of rainfall over time while  $I(S(t))$  is the inflow from irrigation applications.  $ET(S(t), C(t))$  is the coupled water losses from evaporation and transpiration modulated by  $S$  and canopy cover,  $C(t)$ .  $Q(S(t))$  represents the coupled losses from runoff and percolation below the rooting zone  $Z_r$ , and  $dt$  is the integration (delta) time (for full methodological considerations, see (Laio et al., 2001a, Laio et al., 2001b, Porporato et al., 2015, Porporato et al., 2001, Rodriguez-Iturbe et al., 2001)). The simplifying assumptions of this soil-water balance approach were that root growth (not modeled here) is restricted to  $Z_r$ , such that the soil column is relatively uniform in composition and hydraulic redistribution throughout  $Z_r$  allows for water to flow to areas of lower saturation.

Previous soil-water balance models have explored the stochastic nature of precipitation times and depths (Laio et al., 2001a, Laio et al., 2001b, Rodriguez-Iturbe et al., 2001). Here, stochastic precipitation,  $R(t)$ , representing a semi-arid, rain-fed environment was used for model development, where the average precipitation arrival time followed the Poisson distribution (mean arrival time =  $1/21$  day $^{-1}$ ; mean precipitation depth = 0.4 cm), respectively.

The irrigation term,  $I(S(t))$ , represents the irrigation rate as a function of  $S$  and  $t$  depending on the irrigation method (e.g., drip, flood, spray) and decision rule used (i.e., the frequency and volume of desired irrigation applications). The decision rules of the irrigation term require

that an irrigation intervention threshold,  $I_i$ , and target soil moisture level,  $I_t$ , be set (both  $I_i$  and  $I_t$  are expressed as a soil moisture percentage of field capacity). The intervention threshold  $I_i$  indicates the point at which irrigation is induced, while the target soil moisture level  $I_t$  indicates the point at which irrigation will cease once  $S$  reaches or exceeds  $I_t$ . Water applied directly to the surface via drip or flood irrigation become subject to the dynamics of  $S$ , while water applied aerially via sprinkler or pivot irrigation is subject to canopy interception and runoff prior to the  $S$  dynamics in the soil column.

The evapotranspiration rate, ET, was assumed proportional to  $S$  and  $C$ , such that:

$ET(S(t), C(t)) = ET_{lsw} * C(t) * K_{cb} * ET_0$ , where  $ET_{lsw}$  represents the water stress coefficient due to limited soil water availability,  $C(t)$  is canopy cover,  $K_{cb}$  is the basal crop coefficient (after (Allen et al., 1998)), and  $ET_0$  is the potential evapotranspiration, which was calculated using the Hargraeves method to minimize required input data (latitude and monthly mean, maximum and minimum temperatures (Hargreaves, 1975, Hargreaves and Allen, 2003)). The water stress coefficient  $ET_{lsw}$  is given as a function of  $S(t)$ ,

$$ET_{lsw} = \begin{cases} ET_w \frac{S - s_h}{s_w - s_h}, & s_h < S \leq s_w, \\ ET_w + (ET_0 - ET_w) \frac{s - s_w}{s^* - s_w}, & s_w < S \leq s^*, \\ ET_0, & s^* < S \leq 1. \end{cases} \quad (2)$$

where  $S^*$  is the soil moisture value below which plants become stressed and begin stomatal closure,  $s_w$  is the soil moisture value inducing plant wilting point,  $s_h$  is the soil moisture value crossing the plant hydroscopic point beyond which moisture losses cease, and  $ET_w$  is the reduced evapotranspiration rate under wilting conditions (following similar conventions used in (Porporato et al., 2001, Porporato et al., 2005, Laio et al., 2001a, Laio et al., 2001b, Pelak et al., 2017, Rodriguez-Iturbe et al., 2001)). Additionally, evaporation rate,  $E$ , was explicitly

decomposed within ET via an evaporation reduction coefficient that was proportionally scaled to  $C$  (following Pelak et al., 2017), such that  $E(S, C, t) = K_r(S)*(1 - C)*E_b*ET_0(t)$ , (3)

where  $E_b$  is the baseline evaporation coefficient and  $K_r(S)$  is the evaporation reduction coefficient, given by

$$K_r(S) = \begin{cases} 0 & s \leq s_h \\ \frac{s - s_h}{1 - s_h} & s \geq s_h \end{cases} \quad (4)$$

This simplification still captures rates of high and low evaporation as  $S$  approaches full saturation or  $s_h$  and allows for decomposition of ET during earlier or later parts of the growing seasons as dominance shifts from evaporation,  $E$ , to transpiration,  $T$  (a broader discussion of this tradeoff is given in (Pelak et al., 2017). Graphical illustrations of each relationship are shown (Figure 4).

The moisture leakage term,  $Q$ , captures losses from runoff as well as deep percolation. Runoff is modeled as a nonlinear function of  $C$  (Figure 4), while percolation was equal to the hydraulic conductivity, given as

$$K(S) = K_{\text{sat}}*S^d, \quad (5)$$

where  $K$  is the hydraulic conductivity,  $K_{\text{sat}}$  is the saturated hydraulic conductivity, and  $d$  is an empirically derived parameter value (Brooks and Corey, 1964, Rodriguez-Iturbe and Porporato, 2004).

### 2.3. Soil physical and hydraulic conductivity dynamics

In order to capture the effects of soil and crop management factors that influence soil processes, we incorporate the dynamics of porosity,  $n$ , and matric potential,  $\psi_s$ , following Pelak and Porporato Pelak and Porporato, 2019 and Clapp and Hornberger, 1978. The pore size distribution,  $f$ , is modeled as a function of soil pore radius,  $r$ , over time such that

$$dt/dt = d(vf)/dr - mf, \quad (6)$$

where  $v$  is the soil drift term for shrinking pore radii and  $m$  is a source-sink term (gain or loss of pores at given radius,  $r$ ). The integration of the pore size distribution over  $r$  is porosity,  $n$ , follows a power law distribution where

$$n(t) = a(t)r^{-b(t)}dr, \quad (7)$$

where  $a$  is a scaling parameter and  $b_e$  is the power law exponent. The change in radii,  $dr$ , is driven by the  $v$  and  $m$ , defined as

$$v(r, t) = r/(a(t)b(t))*(a(t)b'(t)\ln(r) - a'(t)), \quad (8)$$

and

$$m(r, t) = b'(t)/b(t)*(1 - \ln(r)) - a'(t)/(a(t)b(t)), \quad (9)$$

where the prime-noted variables are the parameters' time-derivatives. Using the same convention as Mualem and Dagan, 1978, Brutsaert, 2005, and Pelak and Porporato, 2019, the matric potential was expressed as

$$\psi_s(s, t) = -(C_s/R_m(t))*s^{-1/(1-b(t))}, \quad (10)$$

where  $C_s$  represents the surface tension of water and  $R_m(t)$  is the maximum effective pore radius. From this, the hydraulic conductivity,  $K_{\text{sat}}$ , may be estimated dynamically using the form

$$K_{\text{sat}}(s, t) = [(\gamma_w^*G_e^*n(t)^2*Rm(t)^2*(1 - b(t))^2]/\mu(3 - b(t))(2 - b(t)) * s^{(4 - 2b(t))/(1 - b(t))}, \quad (11)$$

where  $\gamma_w$  and  $\mu$  are the specific weight and dynamic viscosity of water and  $G_e$  is equal to 1/8 (assuming the Hagen-Poiseuille equation, Brutsaert, 2005).

Following the convention used by Pelak and Porporato, 2019, the power law exponent  $b$  was decomposed into two time-dependent

variables that aim to capture management and landscape changes arising from tillage and consolidation and soil organic matter (SOM) dynamics. Introduction of tillage immediately induces soil pore redistribution closer to uniform pore radii that gradually consolidate over time. Pore consolidation is modeled as an exponential decay function towards the untilled soil pore distribution, expressed as the settling term

$$\gamma_b = r_b + (1 - r_b)*\exp(-k_b(tdd)), \quad (12)$$

where  $\gamma_b$  is the management factor used in the  $b$  term,  $r_b$  is the ratio of the parameter value in an untilled state to the base value,  $k_b$  is the rate of settling, and  $tdd$  is the time since tillage in days. In a cultivated system, tillage resets the soil pore distribution to its initial value since  $tdd$  equals 0.

Although SOM and its turnover cross-cuts many of soil processes influencing soil porosity and hydraulic properties and is likely coupled to landscape management practices, the SOM contribution is treated independently. The function for  $b_c$ , the effect of SOM on the  $b$  term, defined as

$$b_c(OM(t)) = b_0 + \sigma_b OM(t). \quad (13)$$

where  $b_c$  is the parameter value at OM equal to 0 and  $\sigma_b$  is the slope of the  $b$ -OM relationship. Assuming a linear function provides a parsimonious means to incorporating SOM dynamics, however, a nonlinear functional form would likely be more realistic. The  $b$  term then becomes

$$b(tdd, OM(t)) = \gamma_b * b_c, \quad (14)$$

Finally, as porosity  $n$  changes over time, the porosity value feeds back to the affect the water balance in equation 1.

### 2.4. Plant canopy cover dynamics

The plant productivity and canopy cover component consists of a single stock of biomass which accumulates through growth due to ET and diminishes through losses of senescence and physical disturbance through harvesting, livestock grazing, or other management treatments, giving:

$$dC/dt = G(C, S, N, t) - M(C, t) - H(C, t), \quad (15)$$

where  $G$  is the canopy growth rate and  $M$  is the metabolic and senescence term. The growth rate is proportional to nitrogen uptake,  $U$ :

$$G(C, S, N, t) = r_g^*U(C, S, N, t), \quad (16)$$

where  $r_g$  represents a scalar of canopy cover growth per unit of nitrogen utilization. The metabolic and senescence rate,  $M$ , is defined as a function of both constant metabolism and time-dependent senescence terms such that senescence only occurs after the completion of the growing season (i.e., post-plant maturity), described as

$$M(C, t) = (r_m + \gamma(t - t_{\text{sen}})*\Theta(t - t_{\text{sen}}))^*C^2, \quad (17)$$

where  $r_m$  is the metabolic constant,  $t_{\text{sen}}$  is the estimated time of senescence in days,  $\gamma$  is the slope of the senescence curve post- $t_{\text{sen}}$ , and  $\Theta$  is a step function that causes senescence to begin. When soil moisture and nitrogen are non-limiting,  $C$  exhibits patterns of the logistic growth equation (exponential growth followed by leveling off near the maturation canopy level; Hsiao et al., 2009, Liao et al., 2001a, Pelak et al., 2017).

Finally, harvest,  $H$ , is given by

$$H = C^*H_v^*H_d, \quad (18)$$

where  $H$  is initiated at the day of harvest,  $H_d$ , either at the end of the growing season (e.g., for crops) or periodically (e.g., for grazing), with a percentage of biomass removed,  $H_v$ , of canopy,  $C$ .

Canopy that is not harvested becomes soil surface-litter cover based on the fraction of canopy becoming surface material,  $C_{\text{lc}}$ , and time to litter fall,  $C_{\text{lt}}$ . Litter remains is a transient state during the nutrient

turnover process. Therefore, litter turnover,  $LT$  is approximated as  $C_{lc}$  divided by plant litter turnover time,  $C_{lt}$ .  $LT$  reduces the fraction of soil surface coverage and contributes to natural nitrogen deposition, described below.

### 2.5. Soil nitrogen dynamics

Soil nitrogen in the soil column is expressed as the balance between fertilization, deposition, leaching, and plant uptake:

$$dN_c/dt = D(t) + F(N, t) - L(S, N) - U(S, N, C, t), \quad (19)$$

where  $N_c$  is the total mineral nitrogen content level per unit area soil,  $D$  is the natural deposition rate (assumed constant) and  $F$  is the fertilization rate at time  $t$  of fertilizer application. Individual nitrate and ammonium concentrations are not modeled since plants may use both forms of N, simplifying the model N parameterization (a similar convention to [Pelak et al., 2017](#)). Leakage,  $L$ , is proportional to the moisture leakage  $Q$  and the nitrogen concentration at time  $t$ ,

$$L(S, N) = \eta^*Q(S), \quad (20)$$

where  $\eta$  represents the nitrogen content of soil moisture, estimated as  $\eta = aN/SnZ$ ,

where  $a$  represents the dissolved N percentage within the soil column.

Plant uptake,  $U$ , is estimated as

$$U(S, N, C, t) = f(\eta)^*T(S, C, t), \quad (22)$$

where  $f(\eta)$  represents the limitation of nitrogen uptake beyond the critical threshold  $\eta_c$ , which is the point where additional nitrogen uptake does not facilitate increases in plant growth. This takes the form

$$f(\eta) = \begin{cases} \frac{aN}{SnZ} & \frac{aN}{SnZ} < \eta_c \\ \eta_c & \frac{aN}{SnZ} \geq \eta_c \end{cases} \quad (23)$$

Using this parameterization it has been shown that reduction in  $S$  can either facilitate or hinder nitrogen uptake,  $U$  ([Pelak et al., 2017](#)). For example, when  $S > S^*$  and  $\eta < \eta_c$ , reducing  $S$  causes increase in  $U$ ; when  $S < S^*$ ,  $U$  will decrease with the corresponding decrease in ET.

### 2.6. Salinity dynamics

The salt content balance expressed as the number of moles of charge (or equivalent) of cations per unit area is expressed

$$dq_s/dt = IV_i - Q^*V, \quad (24)$$

where  $q_s$  is the salt dissolved in water in the soil column, salt inflow is a function of irrigation applications,  $I$ , with salt concentration  $V_i$ , and the outflow is a function of leakage from the soil column,  $Q$ , and  $V$ , representing the dissolved salt concentration. Salt concentration,  $V$ , can be expressed as  $q_s/w^*$ , where  $w^*$  represents volumetric water content.

Common cations in saline soils include  $\text{Na}^+$ ,  $\text{Ca}^{2+}$ ,  $\text{Mg}^{2+}$ , and  $\text{K}^+$ , subject to adsorption and desorption dynamics. Following [Hsiao et al., 2009](#), we simplify the model consideration to  $\text{Na}^+$  and  $\text{Ca}^{2+}$ . The salt dissolved in water in the soil column,  $q_s$ , may therefore be decomposed to

$$q_s = q_s \text{Na} + q_s \text{Ca}, \quad (25)$$

or on a percentage basis as

$$E_s \text{Na} = q_s \text{Na}/q_s; \quad E_s \text{Ca} = q_s \text{Ca}/q_s, \quad (26)$$

where  $E_s \text{Na} + E_s \text{Ca} = 1$ .

Total charge of dissolved salts may then be described given

$$q_s \text{Na} = C_w^* E_s \text{Na}, \quad (27)$$

$$q_s \text{Ca} = C_w^* E_s \text{Ca}. \quad (28)$$

To account for the cations adsorbed to negatively charged soil

particles, the Cation Exchange Capacity (CEC) is used. The CEC is expressed as

$$CEC = q_x/M = (q_x \text{Na} + q_x \text{Ca})/M \quad (29)$$

where  $x$  denotes cations in the exchange complex and  $M$  is the mass of dry soil to depth  $Z_r$ . The salt quantities in the exchange complex are then expressed as

$$q_x \text{Na} = CEC^* M^* E_x \text{Na} \quad (30)$$

$$q_x \text{Ca} = CEC^* M^* E_x \text{Ca}, \quad (31)$$

where the fraction of sodium in the exchange complex,  $E_x \text{Na}$ , is noted as the Exchangeable Sodium Percentage (ESP), useful for delineating sodicity hazards in a given soil.

The balance between soil water and the exchange complex are assumed to be in thermodynamic equilibrium using the following exchange function for the Exchangeable Sodium Ration (ESR),

$$ESR = K_g SAR, \quad (32)$$

where  $K_g$  represents the Gapon selectivity coefficient and SAR represents the Sodium Adsorption Ratio. The ESR and ESP can therefore be further defined as

$$ESR = E_x \text{Na}/E_x \text{Ca} = (ESP/100)/(1 - ESP/100), \quad (33)$$

$$SAR = \text{Na}/\sqrt{(\text{Ca} + \text{Mg})/2}, \quad (34)$$

which assumes that Ca and Mg are indistinguishable in the exchange complex, following [Mau and Porporato, 2015](#). Inclusion of soil salinity and sodicity is important from an agricultural resource management perspective since accumulation of salts can hinder proper plant functions that lead to productivity. Given the effects of salinity and sodicity on plant productivity ([Allen et al., 1998](#), [Bernstein, 1975](#), [Duncan et al., 2008](#), [Niu and Cabrera, 2010](#), [Qadir and Oster, 2004](#), [Wichelns and Qadir, 2015](#)), the sodium impact on basal crop coefficient was included as a nonlinear table function such that for  $E_x \text{Na}$  or  $ESP$  levels below 0.3 (or 30%) there is no reduction in  $K_{cb}$ . For levels of  $E_x \text{Na}$  between 30% and 100%,  $K_{cb}$  is reduced by 50% ([Figure 4\(d\)](#)).

### 2.7. Crop production and yield dynamics

The endogenous dynamics of the model are coupled through the linkages between  $C$ ,  $S$ ,  $N$ , and  $q_s$ , described above, out of which crop production and yield arise as products of the interactions between the soil-water-plant system. Following the convention of ([Pelak et al., 2017](#)), accumulation of crop biomass,  $B$ , is given as a function of water productivity (driven by transpiration,  $T$ ) along with nitrogen uptake and soil moisture dynamics. Including nitrogen dynamics along with soil moisture availability, which partially drives ET, allows for examination of moisture and nitrogen limitation in tandem, an important coupling in terms of agricultural resource management. The detailed formulation for  $B$  is described as

$$dB/dt = W^* U(S, N, C, t)/\eta_c ET_0(t) = W/\eta_c K_s(S) K_{cb} f(\eta) C. \quad (35)$$

Yield,  $Y$ , was then estimated as a fraction of the biomass using a harvest index,  $h_b$ , giving

$$Y = B^* h_b. \quad (36)$$

### 2.8. Economic dynamics

The economic dynamics account for the input costs and output revenues of the production system. Input costs include fertilizer expenses, dependent on the volume and per unit cost of N, while irrigation includes both fixed and variable costs. Fixed costs of irrigation can vary depending on the method of application, while the variable costs of irrigation are simply the volume of water applied multiplied by the water cost per unit. This captures the trade-off between irrigation

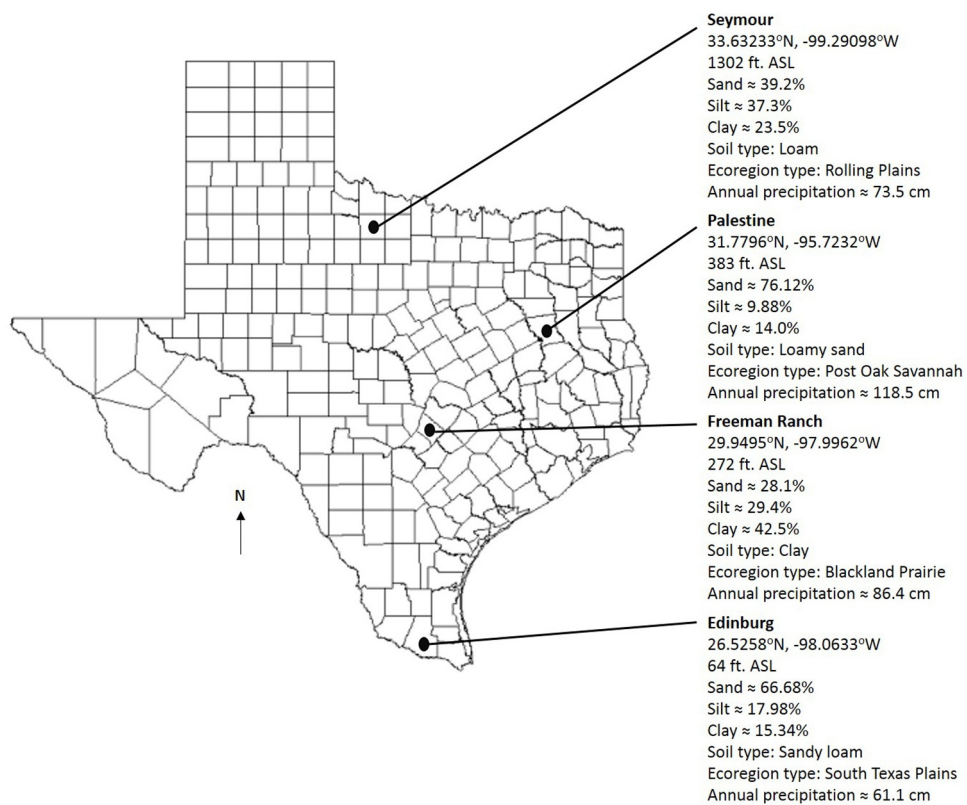


**Figure 5.** Locations in Texas, USA, and their associated geographic, soil, and precipitation characteristics used for model development, calibration, and evaluation against observed data.

systems, where systems with high fixed costs per user (e.g., drip or sprinkler systems), which have lower variable costs due to savings created through lower water requirements, versus systems with lower fixed costs to the user (e.g., flood irrigation) that possess higher variable costs due to higher volumes of water applied. Lastly, revenues are determined using the price per unit of crop,  $P$ , multiplied by the yield,  $Y$ . Returns were then calculated as the difference between revenues and costs.

#### 2.9. Model calibration measurements and model evaluation

In order to calibrate the developed model, soil-moisture data were obtained via the North American Soil Moisture Database (Quiring et al., 2016) for four locations in the state of Texas, USA (Figure 5), representing contrasting soil, ecoregional, climatic and precipitation regimes, and irrigation capabilities (Table 1). Initial  $S$  was set to the initial soil moisture level for an observation year containing up to 365 days. Climate data needed for precipitation forcing and Hargreaves ET<sub>0</sub> calculations were downloaded from Weather Underground ([wunderground.com](http://wunderground.com)) for each location. Since precipitation data were obtained in proximity to and not directly at the locations where soil moisture was recorded, an adjustment had to be made for clear outlier precipitation events that did occur in the general area but did not occur at the specific soil monitoring point. In total, precipitation events had to be reduced or eliminated for 27 days (out of a total 1460 days, or 365 days for each of the 4 locations), or 1.8% of the total simulation days. After accounting for these events, calibration measurements were taken for metrics of model accuracy (Mean Bias), precision (coefficient of determination,  $r^2$ ), and overall fit (Theil inequality measures) for each site, following model evaluation considerations of Tedeschi (Tedeschi, 2005) and Oliva (Oliva, 1995). Theil inequality analysis decomposes the total model error into errors attributable to discrepancies in the mean, variance, and covariance's of predicted and observed values. Generally,

lower Theil values for mean and variance are preferable to higher values (i.e., the model captures the general patterns of behavior and where less emphasis is needed on point estimates that would achieve high agreement in covariance estimates). However, in the case of soil moisture, errors in covariance should be considered given the stochastic nature of hydroclimate forcing at each particular location.

Additional calibration checks were made using the other core state variables of the model, namely canopy-soil cover, soil nitrogen and salinity content, and the critical soil physical and hydraulic properties, including porosity, saturated conductivity, and soil matric potential. In order to evaluate the model's adequacy to replicate behavior patterns and structures in these variables but without data corresponding to the soil moisture monitoring locations, we calibrate the model by running a hypothetical crop growing season with similar soils and parameter values as those found in the literature where observed data were used in model development. In these cases, model simulations of a growing season were compared to model outputs for soil moisture, crop canopy cover, nitrogen, biomass and yield dynamics (Pelak et al., 2017), and soil porosity and pore radii (Pelak and Porporato, 2019). To examine the adequacy of underlying soil processes, sensitivity analyses were run to examine the behavior of soil salinity to altering irrigation and leakage rates (similar to Mau and Porporato, 2015), or for alternative soil moisture levels that drive saturated hydraulic conductivity and soil matric potential (similar to Pelak and Porporato, 2019). In the former, irrigation and leakage rates were set to constant levels while salinity was allowed to vary, while in the latter case, soil moisture as a percentage of field capacity was varied from 0 to 100 percent and conductivity and matric potential responses were recorded.

#### 2.10. Sensitivity analyses

After examining the calibration performance for each site, the model was returned to its generic soil characteristics used during model

**Table 1**

Summary of parameter and model structure changes used to facilitate sensitivity analysis, including the input variables or functions, initial parameterized values, values or model modifications used during sensitivity analyses, and the nature of the simulation runs completed.

| Input functions  | Initial parameterization                    | Sensitivity values or model adjustment  | Sensitivity runs |
|--|---|---|------------------|
| <b>Precipitation</b>                                       |   |   |                  |
| Frequency (1/day)  | 1/40  | +/-25%  | n = 1000         |
| Depth (cm)   | 0.5   | +/-25%  |                  |
| <b>Irrigation</b>  |   |   |                  |
| electrolyte concentration in irrigation water (mmol/L)     | 20  | +/-25%  | n = 1000         |
| soil moisture level inducing irrigation applications       | 40% of field capacity                       | +/-25%  |                  |
| target soil moisture level ceasing irrigation applications | 60% of field capacity                       | +/-25%  |                  |
| application interval (days)                                | 10  | +/-25%  |                  |
| <b>Crop management</b>                                     |   |   |                  |
| fertilization (kg/m <sup>2</sup> )                         | 0.011                                       | +/- 0.003   | individual runs  |
| subsurface compaction under tillage                        | porosity, 0.43                              | 0.215   | individual runs  |
| residue management under no-tillage                        | 100% of crop biomass harvested              | 50% of crop biomass harvested   | individual runs  |
| cover cropping under no-tillage                            | no canopy growth outside the growing season | possible canopy growth year round   | individual runs  |
| tile drainage  | none  | additional outflow from soil moisture stock at depth of 45c m and tile drain diameter of 7.5c m | individual runs  |

development representing an agricultural soil similar to Pelak et al., (Pelak et al., 2017) for a variety of sensitivity analyses. The objective of these tests were to examine the response patterns or characteristics of key model structures to varying parameter value changes representing alternative management schemes. In doing so, identification of parameters contributing to significant responses in model state variables is possible while simultaneously insuring the model did not produce any physically unrealistic results (e.g., negative soil moisture levels). Results of sensitivity simulations were compared to the base model results using the statistical screening approach (Ford and Flynn, 2005), where variations in input values are correlated to output responses for each time step, t. This yields an estimate of correlation coefficient, r (which can take on values from -1 to 1), at each time step, making it capable of evaluating the relative strength that each input variable exerts on the output variable over the length of the simulation, a useful approach for evaluating the feedback loop strength that the input variables regulate (and potential shifting dominance). For example, negative correlation values indicate a negative or opposite polarity between input and output variables (i.e., reductions in the input lead to increases in the output). On the other hand, positive correlation values indicate a positive or reinforcing polarity (i.e., increases in one variable lead to still greater increases in another). Values closer to -1 indicate perfect negative polarity, while values nearer to +1 indicate perfect positive polarity. If the coefficient of determination between the input and output variables shifts from negative to positive, a shift in polarity may have occurred.

Whereas several other works have examined the sensitivity of exogenous management inputs such as irrigation or fertilization (Pelak et al., 2017) or endogenous factors such as salinity equations (Mau and Porporato, 2015), here we present sensitivity analyses of critical climate features, primarily precipitation, or management features that influence the soil column that have not been well examined in previous modeling work. To complete the sensitivity analyses, several assumptions were made. For the climate test, namely alteration of precipitation depth and frequencies, we assumed no irrigation to take place in order to examine the response in crop water irrigation requirements from changing precipitation patterns. Altering frequency and depth of precipitation (+/- 25% from their base values of 1 per 40 days for mean event arrival time and 0.5c m for mean depth, respectively) provided a pragmatic way to evaluate soil moisture dynamics and the plant canopy productivity it supports, as well as the derived irrigation demand (i.e., the estimated irrigation demand for crops that would have been demanded given a particular management strategy).

The hypothetical irrigation system used from comparison was a sprinkler irrigation system (subject to canopy interception and runoff dynamics), where a relative soil moisture value of 40% of field capacity would induce irrigation applications up to the target relative soil moisture value of 60% of field capacity, irrigation application intervals up to 10 days and no flush applications would be applied after the growing season. For the remaining management tests, we assume that such an irrigation scheme is in use while we vary salinity and crop management factors. Each test is described below (and summarized in Table 1).

Irrigation management factors, namely electrolyte concentration of irrigation applications, the soil moisture level inducing irrigation application, the target soil moisture level at which irrigation applications cease, and the application interval (base value equal to 10 days) were varied from the base irrigation scheme (just described) by +/25% of their initial base values.

Additionally, several important crop management factors were also tested. Fertilization is a significant agroecosystem input as it facilitates crop growth but is also a source of significant economic and environmental cost (through leakage and runoff). To examine the tradeoff between fertilization costs and benefits, fertilization was varied +/-50% in fertilization rate (assuming 1 application at the beginning of the growing season). Similar to fertilization, tillage is an important management practice since it increases soil microporosity and provides a large nutrient release at crop planting. However, consecutive tillage in the longer-term can lead to subsurface compaction from increasing equipment traffic in the field. To test the model sensitivity to potential compaction from excessive tillage, we vary the soil porosity via a 50% reduction in the initial porosity value. Alternative soil management practices such as no-tillage system that reduce soil disturbance are generally compensated for by the ability to better manage crop residue on the soil surface as well as implement cover cropping systems. We therefore examined the impact of no-tillage through the incorporation of crop residue management (via reduction in canopy removal at time of crop harvest from 100% of crop biomass to 50%) as well as implementation of non-irrigated cover crops (via allowance of plant canopy growth outside of the ordinary growing season).

Finally, an increasingly important management practice has been the installation of tile drainage networks to remove water where soils are subject to periodic saturation due to rising water tables, a function of snowmelt dynamics but primarily the proximity to low lying wetlands. We tested the impact of subsurface tile drainage installation via an additional outflow from the soil column representing tile drain

**Table 2**  
Summary of calibration and statistical measures used for model evaluation.

| Site      | Coefficient of Determination, $r^2$ | Mean Bias (% soil moisture) | Theil Values |       |       |
|-----------|-------------------------------------|-----------------------------|--------------|-------|-------|
|           |                                     |                             | $U_m$        | $U_s$ | $U_c$ |
| Edinburg  | 0.61                                | 0.013                       | 0.39         | 0.19  | 0.58  |
| Freeman   | 0.54                                | 0.027                       | 0.23         | 0.16  | 0.60  |
| Ranch*    |                                     |                             |              |       |       |
| Palestine | 0.79                                | -0.007                      | 0.04         | 0.00  | 0.96  |
| Seymour   | 0.72                                | -0.001                      | 0.00         | 0.04  | 0.96  |

\*n = 290 rather than 365

releases, where the tile was installed at a depth of 45 cm with a 7.5 cm diameter. In this case, the irrigation system is removed since moisture is typically excessive due to water table rises (incorporated via capillary rise of 0.05 cm per day to represent these alternative soil moisture inflows that necessitate drainage). Each of these sensitivity simulations provided a means of evaluating model performance while simultaneously gleaned important insights regarding the potential impact that individual alternative management strategies may have on the overall soil moisture and nutrient dynamics arising from common agroecosystems (via quantifying strength of influence of input parameters on output variables through statistical screening (Ford and Flynn, 2005).

### 3. Results

#### 3.1. Calibration results

Overall, the model was adequately replicated the soil moisture evolution under varying soil physical and climatic conditions (Table 2 and Figure 6). Accuracy, measured by mean bias (in soil moisture percentage terms) was extremely high (mean of 0.008%), and precision estimates were excellent for two sites (Edinburg and Palestine), fair for one site (Seymour), and low for one site that did not have a representative 365 day sample (Freeman Ranch; mean  $r^2$  value given all sites = 0.67). Behavior-over-time graphs for the model generated data compared to observed soil moisture levels as well as the evolution of each Theil Inequality Statistic are provided (Figure 6). The noteworthy discrepancies between observations and model predictions for each specific site are discussed below.

The major errors associated with the Edinburg and Freeman Ranch simulations occurred later in the simulation. In Edinburg, this began with several precipitation events occurring at different days between day 240 and 310. After day 275, the model simulated soil moisture did not decline at as rapid a rate as the observed time series, indicating that moisture losses (or outflows) were smaller in the model than in the real world. This was likely due in part to the timing of precipitation events but also to the specification of soil evaporation for the ending months at this site was too low. Because of this, the contribution of errors in mean to total model errors rose sharply until the end of the simulation period (or growing season). Data for the Freeman Ranch were the scarcest, leading to fewer days of allowable comparison. For the days we did compare, discrepancies indicated that the observed and predicted time-series both peak at similar points corresponding to precipitation events, the slope of the recession limb post precipitation was much steeper in the observed data, indicating that the outflows in the model may not be increasing at the appropriate rate, especially near the end of the simulation (or growing season, similar to the Edinburg location). The results of the Edinburg and Freeman Ranch simulations illustrated a) the trade-off between accuracy of the mean and covariance estimates that arise in any simulation; and b) evapotranspiration demand is likely higher at this site at the end of the year due to other environmental factors not included in the model.

Both the Palestine and Seymour simulations showed high agreement with the observed dynamics of those locations. Unlike the previous two

sites, where the moisture outflows were not high enough to 'drain' the soil moisture stock as quickly as the observed record, the outflows for the Palestine and Seymour cases seem to be very well matched (i.e., similar moisture regression slopes regardless of precipitation event). The Palestine and Seymour simulations appeared to be the best behaved compared to the observed data, but several discrepancies may be found in either case. In the Palestine site, peaks of soil moisture tend to be somewhat lower or higher compared to the historical data while the slope of soil moisture drawdowns remain consistent. Therefore, the major errors associated with this run were likely the mismatch between location of precipitation events driving the soil moisture as well as parameterization of infiltration and runoff, but given the overall estimates for errors in the mean and variance, such improvements may not yield significant gains in model performance. The Seymour site appears to be the model that is the best behaved. Most of the error resides in the covariance fraction. Comparing the observed and predicted data, there are some discrepancies between the timing of precipitation events relevant to the site (e.g., days 57-85; days 183-211; etc.). There is likely minimal parameterization improvements needed for the Seymour model other than having a precipitation record closer to the soil observation point.

Importantly, the integrated model was able to replicate behavior patterns in critical state variables across model components for a hypothetical crop growing season (Figure 7). Soil moisture evolution response to a given precipitation and irrigation sequence (Figure 7a) exhibited similar correspondence a similar ecohydrologic model, while crop canopy cover exhibited logistic growth patterns (Figure 7b; planting time = 120 days) similar to Pelak et al., (Pelak et al., 2017). Tillage, which generally occurs just prior to crop planting dates, created additional pore space via increase soil pore radii (Figure 7c and d), which gradually collapsed over the growing season as soil properties revert back to pre-tillage conditions (Pelak and Porporato, 2019). Nitrogen uptake (Figure 7e) mimicked crop canopy, since nitrogen fuels accelerated crop growth up to the point of maturity, at which time nutrient uptake begins to decline (Pelak et al., 2017), while crop biomass and yield continue to grow until harvest (harvest time = 270 days; Figure 7f). Meanwhile, salt concentration accumulated in the soil column driven by irrigation rate and leach fraction (defined as the fraction of irrigation applications that infiltrate below the rooting zone) expressed similar nonlinear behaviors as Mau and Porporato (Mau and Porporato, 2015) (Figure 7g). Additionally, varying soil moisture levels had the appropriate response on hydraulic conductivity (Figure 8a) and matric potential (Figure 8b).

#### 3.2. Sensitivity analyses

##### 3.2.1. Precipitation frequency and depth

The purpose of the precipitation sensitivity test was to evaluate the robustness of the model to alternative values of precipitation by varying mean rainfall arrival times and depths. The precipitation sensitivity test had large, significant effects on soil moisture and therefore the derived irrigation demand (Figure 9). In this particular test, rainfall was varied from its parameterization of a semi-arid precipitation regime up to very humid or down to extremely arid regimes, evidenced by the large variation in soil moisture (Figure 9a). Of the two factors, arrival time had a higher correlation  $r$  compared to precipitation depth (0.52 vs 0.24; Table 3 and Figure 9b), indicating that precipitation mean arrival time was more influential in regulating higher soil moisture levels than mean precipitation depths. The same effect was also observed in average soil moisture (Figure 9c and d). In terms of derived irrigation demand, the mean volume of irrigation that would have been demanded (assuming spray irrigation induced at 40% of field capacity, continuing until the target soil moisture level of 60% of field capacity is reached) was 110 cm (Figure 9e). Similar to the soil moisture estimates, frequency or mean arrival time was more influential than mean precipitation depth (i.e., as mean arrival time was shortened, derived

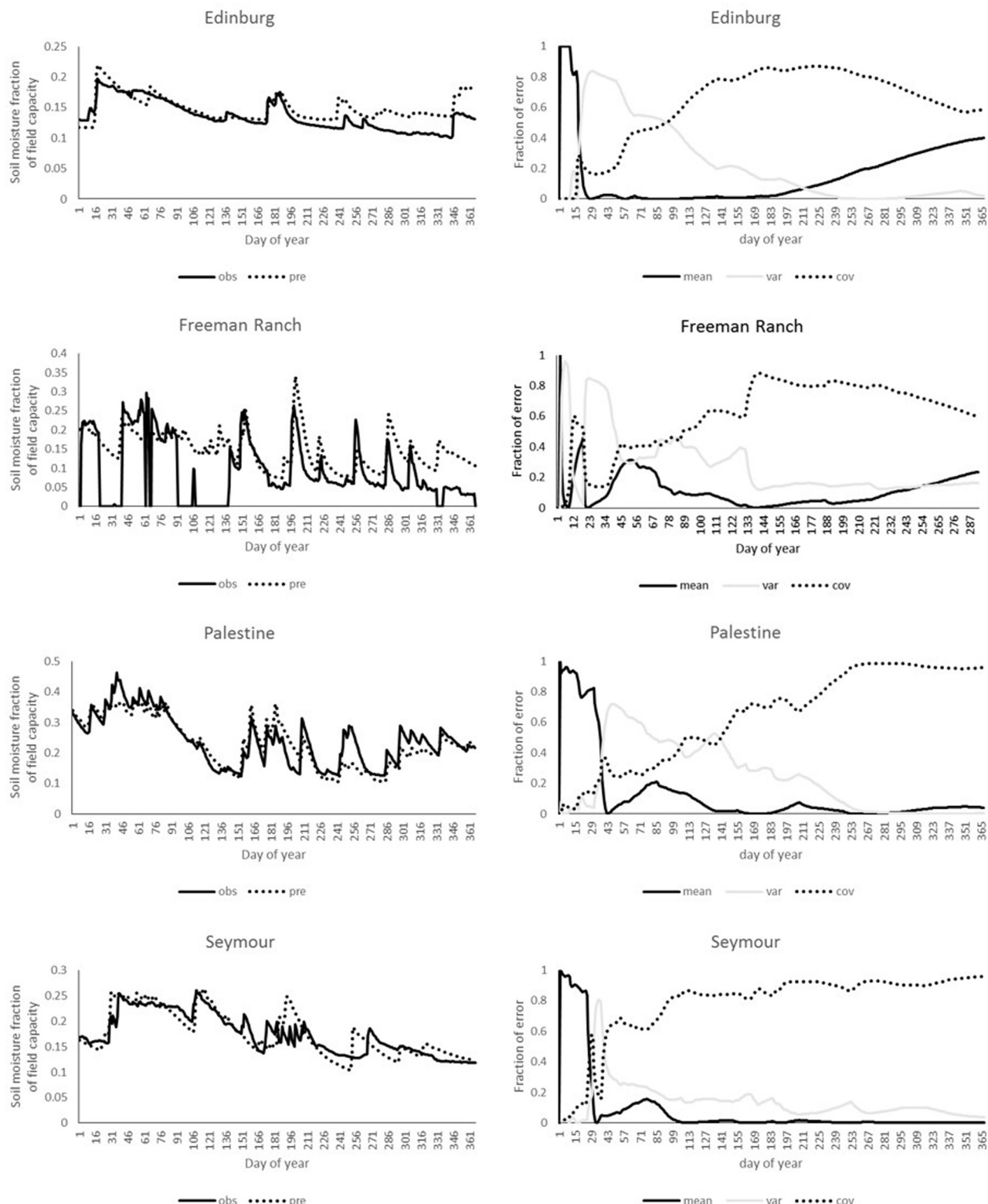


**Figure 6.** Behavior-over-time graphs in soil moisture evolution at each site (left panel) displaying observed (obs) and model predicted (pre) soil moisture expressed as a fraction of the soil field capacity, alongside the evolution of Theil Inequality Statistics (i.e., percentage of the model's error term arising from differences in observed and predicted mean, variance, and covariance; right panel) for each of the four sites.

irrigation demand decreased; Table 3, Figure 9f).

### 3.2.2. Irrigation management tests

The purpose of the irrigation management sensitivity test was to evaluate the probable responses of key system characteristics to altered

irrigation management criteria: irrigation threshold (i.e., the soil moisture level that induces irrigation applications), the electrolyte concentration of each irrigation application, the irrigation interval (i.e., days between applications), and the target soil moisture level that ceases applications. Altered behavior patterns in response variables are

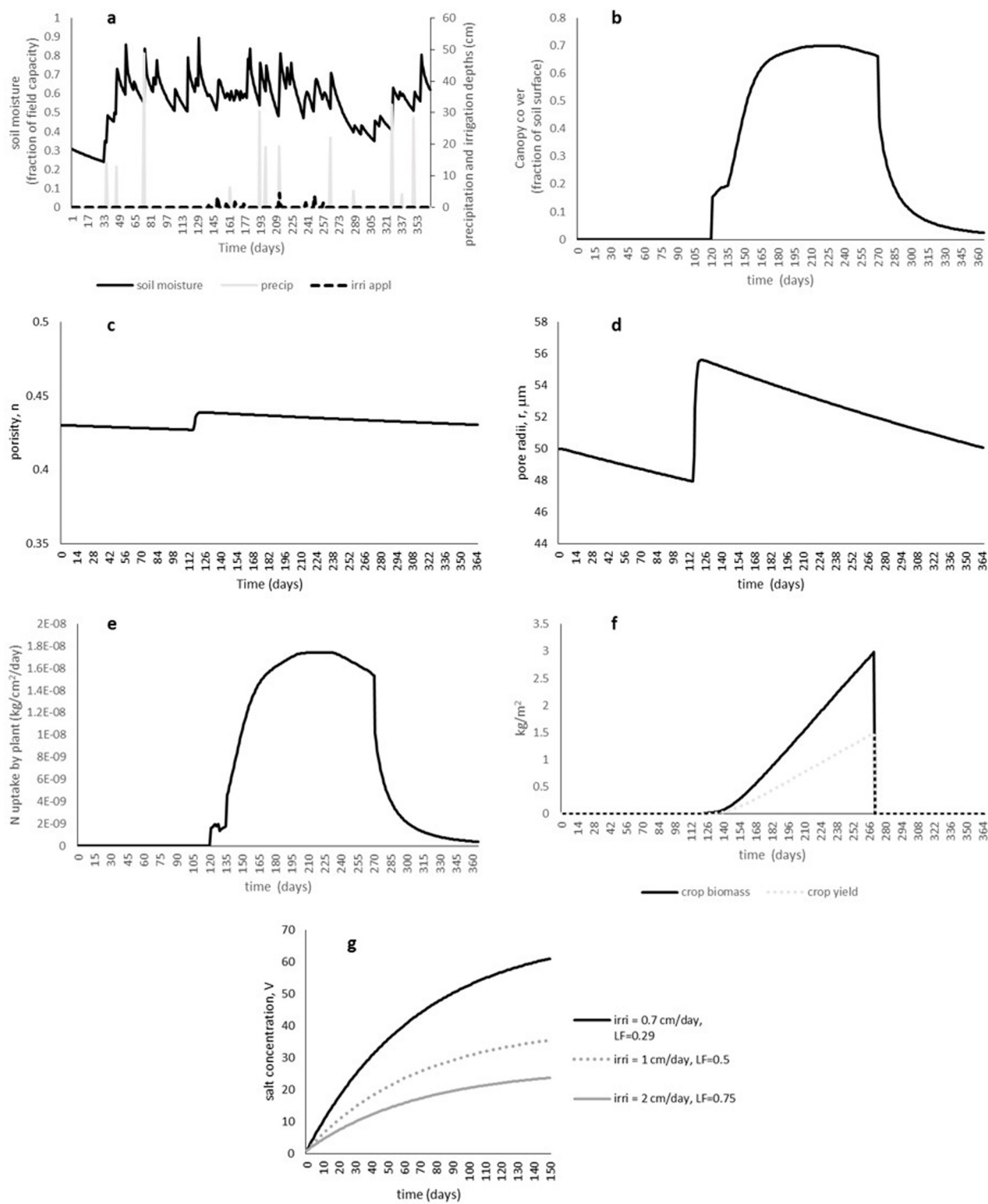


**Figure 7.** Summary table of sensitivity results from each management test. Mean values at the end of test simulation (day 365) are shown with the percentage difference from the base case below. Given the -1.9% mean bias in model generated data for soil moisture (Table 2) that drives the remaining dynamics, values resulting in absolute value of percentage differences greater than the base case, denoted \*, indicate the given test created significant behavioral differences from the base case.

shown in Figure 10 while ending CC values between input value changes and responses in model are shown in Table 3. No changes in soil moisture occur until the start of the growing season and irrigation applications begin near day 120 (Figure 10a). The majority of simulations occurred within +/-25% of the mean soil moisture level.

Depending on the particular input combination, cumulative irrigation ranged between 25 and 40 cm, with the majority of simulations occurring within +/-33% of the mean irrigation level (Figure 10b). Although canopy cover varied throughout the growing season in response to moisture availability, the ending canopy cover values were within

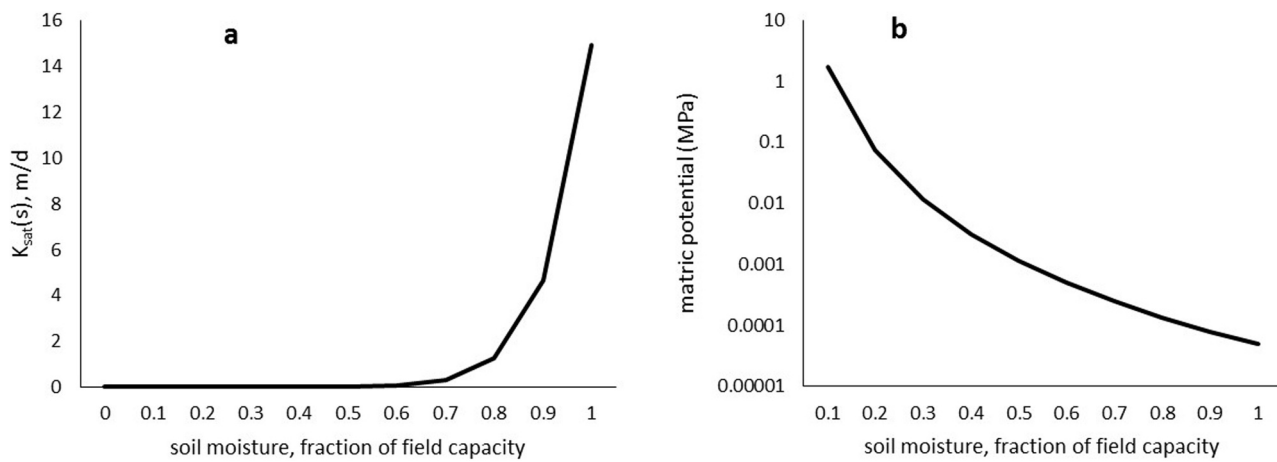


**Figure 8.** Replication of empirical non-linear relationships from model outputs for hydraulic conductivity (panel a) and matric potential (panel b).

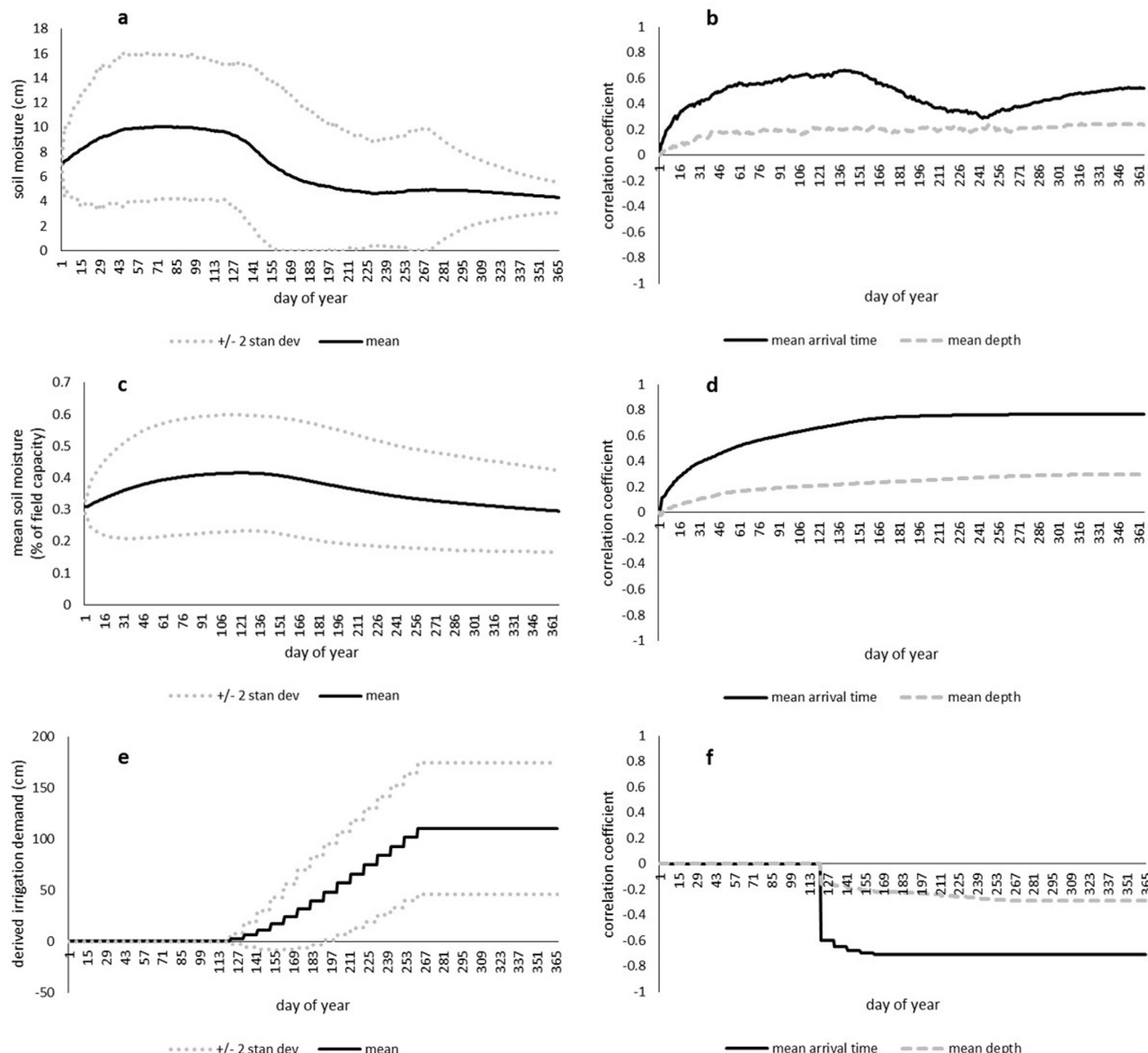


**Figure 9.** Sensitivity plots for precipitation sensitivity runs ( $n=1000$  simulations, left-side panels) and the associated behaviors in correlation coefficients between mean precipitation arrival times and depths indicating strength of precipitation parameters on resulting dynamics (right side panels) for soil moisture evolution (panels a and b), mean soil moisture (panels c and d), and derived irrigation demand (panels e and f).

**Table 3**

Summary table of sensitivity results from the precipitation and irrigation tests. Reported values are the ending correlation coefficients (CC) between the input function and the model parameter. Positive CC values indicate positive/reinforcing polarity (i.e., increasing the input values led to increases in the model output), while negative CC values indicate negative/opposite polarity (i.e., increasing the input variable led to decreases in the model output). Values closer to absolute value 1 indicate stronger influence, while values closer to 0 indicate a weaker influence.

| Input functions  | annual profit | canopy cover | derived irrigation demand | cumulative irrigation | soil moisture | salt concentration | average soil moisture | soil moisture percentage of field capacity | yield |
|--|---------------|--------------|---------------------------|-----------------------|---------------|--------------------|-----------------------|--|-------|
| <b>Precipitation</b>                                       |               |              |                           |                       |               |                    |                       |  |       |
| Frequency (1/day)  | 0.77          | -0.38        | -0.71                     | -                     | 0.52          | -0.40              | 0.77                  | 0.52                                       | -0.40 |
| Depth (cm)   | 0.17          | -0.08        | -0.29                     | -                     | 0.24          | -0.24              | 0.30                  | 0.24                                       | -0.09 |
| <b>Irrigation</b>  |               |              |                           |                       |               |                    |                       |  |       |
| soil moisture level inducing irrigation applications       | -0.44         | 0.40         | -                         | 0.44                  | 0.44          | 0.29               | 0.59                  | 0.44                                       | 0.33  |
| electrolyte concentration in irrigation water (mmol/L)     | -0.03         | 0.05         | -                         | 0.05                  | 0.06          | 0.81               | 0.05                  | 0.06                                       | 0.05  |
| application interval (days)                                | 0.09          | -0.10        | -                         | -0.11                 | -0.11         | -0.07              | -0.13                 | -0.11                                      | -0.09 |
| target soil moisture level ceasing irrigation applications | -0.83         | 0.05         | -                         | 0.75                  | 0.29          | 0.45               | 0.72                  | 0.29                                       | 0.01  |

10% of the mean cover (Figure 10c). Electrolyte concentration, a function of irrigation applications and the salt concentration therein, mimicked the response of cumulative irrigation (Figure 10d). Because of the irrigation strategy maintained soil moisture levels greater than what would have been achieved without it, both mean soil moisture (Figure 10e) and yield (Figure 10f) showed less variability than did the other parameters.

Of the irrigation sensitivity parameters, irrigation threshold had the strongest influence on soil moisture ( $CC = 0.44$ ) and yield ( $CC = 0.33$ ) (Table 3), since raising irrigation threshold would induce irrigation applications earlier, reducing the likelihood of soil moisture becoming a crop growth limiting factor. However, a trade-off was observed between soil moisture and yield with profit, since increased irrigation threshold created greater irrigation applications ( $CC = 0.44$ ), which led to increased costs that necessarily reduced profits ( $CC = -0.44$ ). Similarly, raising the target soil moisture level led to increased irrigation levels ( $CC = 0.75$ ) and therefore costs, which profitability ( $CC = -0.83$ ) (Table 3). Electrolyte concentration in irrigation water had little impact on soil and crop parameters except for the soil salt concentration (0.81) at the end of the growing season. The influence of irrigation application interval (days) was consistent across soil and crop factors (with CC values ranging from 0.09 to 0.13) but did not as significantly influence any particular factor as the other irrigation parameters (Table 3).

### 3.2.3. Crop management tests

The purpose of the crop management sensitivity tests was to evaluate changes in soil and crop system behaviors to alternative management practices employed in various agroecosystems. The most common of these practices is fertilization. Reducing fertilization rates 50% from the base case ( $0.011 \text{ kg/m}^2$ ) led to reduced crop transpiration, yield and profit (Figure 11). Because of the reduced transpiration, mean soil moisture was higher than in the base case (Table 4). On the other hand, increasing fertilization led to greater transpiration (due to crop growth rates unhindered by nutrient availability), yield and profit (Figure 11), with a corresponding decrease in mean soil moisture (Table 4).

The influence of tillage, if excessive to the point to create a compacted subsurface soil column, significantly reduced soil moisture (Figure 12a), infiltration rates (Figure 12b), mean soil moisture, yields, and profits (Table 4).

Two no-till scenarios, one with crop residue management and one with non-irrigated cover crops, revealed divergent dynamics (Table 4). Incorporation of crop residue increased soil moisture levels 10.7% over the base case (Figure 12c) compared to the cover crop scenario of 0.79%, respectively (Figure 12e). This was due in large part to the increased transpiration, canopy cover, and yield under the cover crop scenario that was not present in the crop residue scenario (Table 4; Figure 12d and f).

For those systems where excessive moisture becomes a problem, installation of tile drainage is a common practice used to manage water in the soil column. The tile drainage scenario, which did not include irrigation due to excessive moisture of rising water tables, did reduce soil moisture as well as the evapotranspiration dynamics (Table 4; Figure 12g). Although yield and profitability were also reduced compared to the base case, in reality where these soils necessitating drainage exist, yield and profitability prior to drainage are effectively zero. Therefore, the percentage changes for yield and profit under drainage are not shown – so long as the annualized cost of tile drain installation does not outweigh expected crop profit margins per unit area, it would be economically justifiable to tile (Table 4).

The resulting evapotranspiration dynamics for each of the crop management tests revealed unique evolutions in the soil water balance (Figure 13). Although the peaks rates of ET under compaction were similar to that of the no-till scenarios, it was also more variable (Figure 13a), contributing to lower yields and profits (Table 4). Between the no-till scenarios, managing for crop residue produced greater mean soil moisture compared to cover cropping (Table 4), since ET was

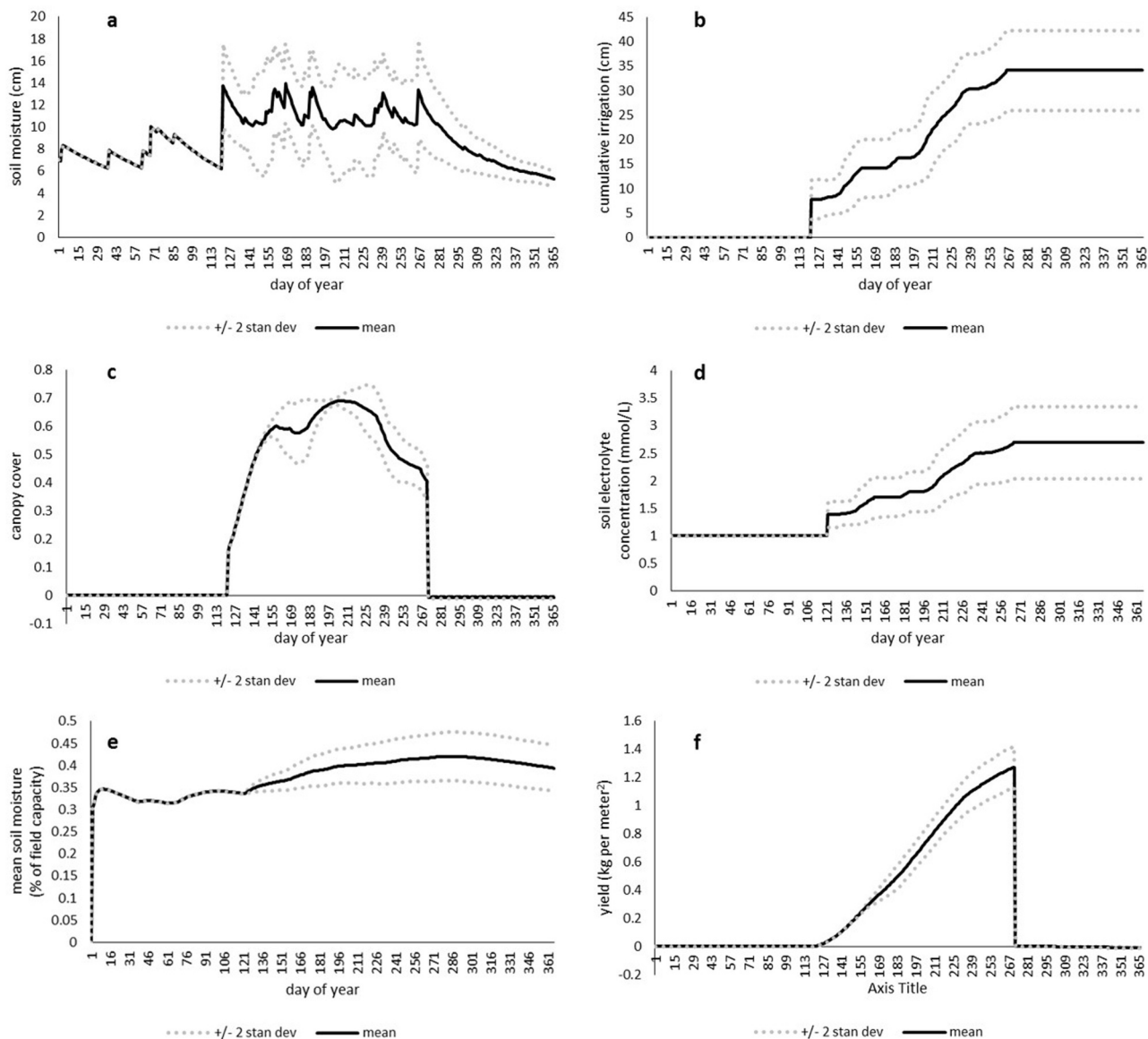


**Figure 10.** Sensitivity plots for the irrigation management sensitivity trials ( $n=1000$  simulations) in which the soil moisture level inducing irrigation (irrigation threshold), the electrolyte concentration in irrigation water, the irrigation interval, and the target soil moisture level were varied, illustrating the mean response and  $+/ -$  two standard deviations from the mean for soil moisture (panel a), cumulative irrigation (panel b), canopy cover (panel c), soil electrolyte concentration (panel d), mean soil moisture (panel e), and crop yield (panel f).

significantly less during times of the year outside of the growing season (Figure 13b) compared to the cover crop, whose transpiration rate year round (Figure 13c) drew down soil moisture levels. Finally, the influence of tile drainage created a unique soil moisture evolution given rising water tables (Figure 13d). With drainage, soil moisture was maintained near its average condition, which constrained ET both within and outside of the growing season.

#### 4. Discussion

Soil systems form the foundation of agroecosystems that society relies on for the production of food, feed, and bioenergy, and as such, the functioning of soil processes are critical for meeting the growing demands of population growth. As agricultural production attempts to expand via both intensification (i.e., increasing efficiency and productivity on existing agricultural lands) and extensification (i.e., increasing the land use devoted to agriculture), soil functions and processes will become increasingly stressed due to a number of unintended

consequences, such as erosion, reduction in water holding capacity, loss of soil organic carbon, excessive fertilization and water runoff contamination, and soil salinization, among other externalities. Variability in hydro-climate forcing adds to the already complex nature and behavior of soil systems.

This paper presented a soil system dynamics model, grounded in soil moisture dynamics applications stemming from the field of ecohydrology, that demonstrated the ability to integrate soil water and nutrient processes and cross-cut multiple agroecosystem management strategies, primarily irrigation, fertilization, and crop management techniques including cover cropping and various tillage practices. The model included core state variables for soil moisture, nitrogen, and salinity, crop canopy cover and soil ground cover, and crop system profitability. The relationships between these components were quantified and parameterized using parsimonious assumptions and leveraging existing ecohydrologic modeling frameworks from a multitude of sources. The calibration results efficiently replicated observed soil moisture dynamics for a variety of soil types, while other measures or

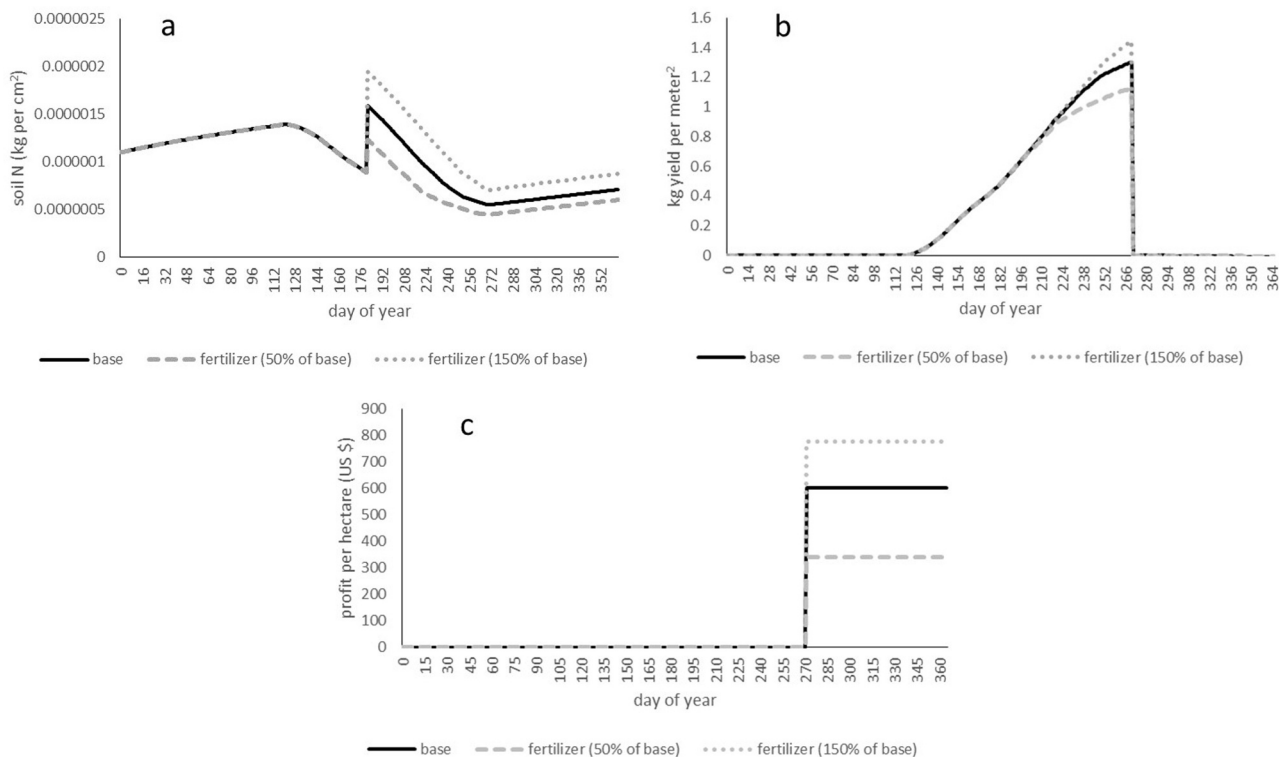


**Figure 11.** Resulting dynamics of the fertilizer sensitivity test (+/-50% of the base fertilizer rate of  $0.011 \text{ kg m}^{-2}$ ) on soil nitrogen content (panel a), crop yield (panel b), and profitability (panel c).

relationships (e.g., nitrogen dynamics, canopy cover, soil hydraulic conductivity and matric potential) produced by the model matched extremely closely to observed or modeled expectations in the literature.

Using a variety of model tests, we examined the response in soil system behaviors to varying precipitation, irrigation, and crop management factors to identify critical feedback linkages between system components. Some of the response patterns were expected and build additional confidence in the model structure. For example, increasing frequency and depth of precipitation reduced irrigation demand (and therefore costs), increased mean soil moisture and yields, resulting in improved profitability. On the other hand, altering irrigation decision parameters resulted in important soil resource and economic outcomes. Reducing the soil moisture level that induces irrigation and the target soil moisture level led to similar reductions in soil moisture and yield (of the two, the soil moisture level inducing irrigation was more significant), but increased profitability due to the reduced irrigation costs.

These effects help up regardless of irrigation application interval, implying that moisture levels inducing irrigation applications be set as low as possible (e.g., near to  $s^*$ ) and that the target soil moisture level be determined by the ease of application (e.g., just above  $s^*$  for drip- or micro-irrigation systems or  $s_{fc}$  for spray or flood irrigation systems). Although previous model studies focused less on the type of irrigation system, the convergence on  $s^*$  as an optimal point was also identified by Pelak et al., 2017.

Specifically regarding crop management tests, increasing or decreasing fertilization rate led to corresponding increases or decreases in soil moisture, driven by the changes in transpiration (greater fertilization led to greater crop biomass, which transpired more moisture). Or consider soil compaction, a common symptom impacting many agroecosystems due to excessive surface disturbances that compress soil pore space. Under the soil compaction test, significant reductions were observed in mean soil moisture, evapotranspiration dynamics, yield, and

**Table 4**

Summary table of sensitivity results from each management test. Mean values at the end of test simulation (day 365) are shown with the percentage difference from the base case below. Given the -1.9% mean bias in model generated data for soil moisture (Table 3) that drives the remaining dynamics, values resulting in absolute value of percentage differences greater than the base case, denoted \*, indicate the given test created significant behavioral differences from the base case.

| Test                             | mean soil moisture (cm) | cumulative E (cm) | cumulative T (cm) | yield ( $\text{kg m}^{-2}$ ) | profit (\$/ha) |
|----------------------------------|-------------------------|-------------------|-------------------|------------------------------|----------------|
| base                             | 8.88                    | 29.38             | 37.00             | 1.30                         | 600.92         |
| fertilization rate (-50%)        | 9.19*                   | 32.51*            | 34.27*            | 1.12*                        | 339.01*        |
|                                  | 3.49%                   | 10.65%            | -7.38%            | -13.85%                      | -43.58%        |
| fertilization rate (+ 50%)       | 8.78                    | 27.88*            | 38.74*            | 1.44*                        | 777.25*        |
|                                  | -1.13%                  | -5.11%            | 4.70%             | 10.77%                       | 29.34%         |
| compaction                       | 4.70*                   | 32.07*            | 36.60             | 1.27*                        | 564.64*        |
|                                  | -47.07%                 | 9.16%             | -1.08%            | -2.31%                       | -6.04%         |
| no-till, with residue management | 9.83*                   | 33.90*            | 41.90*            | 1.43*                        | 722.40*        |
|                                  | 10.70%                  | 15.38%            | 13.24%            | 10.00%                       | 20.22%         |
| no-till, with cover cropping     | 8.95                    | 24.70*            | 56.58*            | 1.78*                        | 1156.90*       |
|                                  | 0.79%                   | -15.93%           | 52.92%            | 36.92%                       | 92.52%         |
| tile drainage                    | 5.81*                   | 23.80*            | 22.19*            | 1.11*                        | 1367.61*       |
|                                  | -34.57%                 | -18.99%           | -40.03%           | -14.62%                      | 127.59%        |

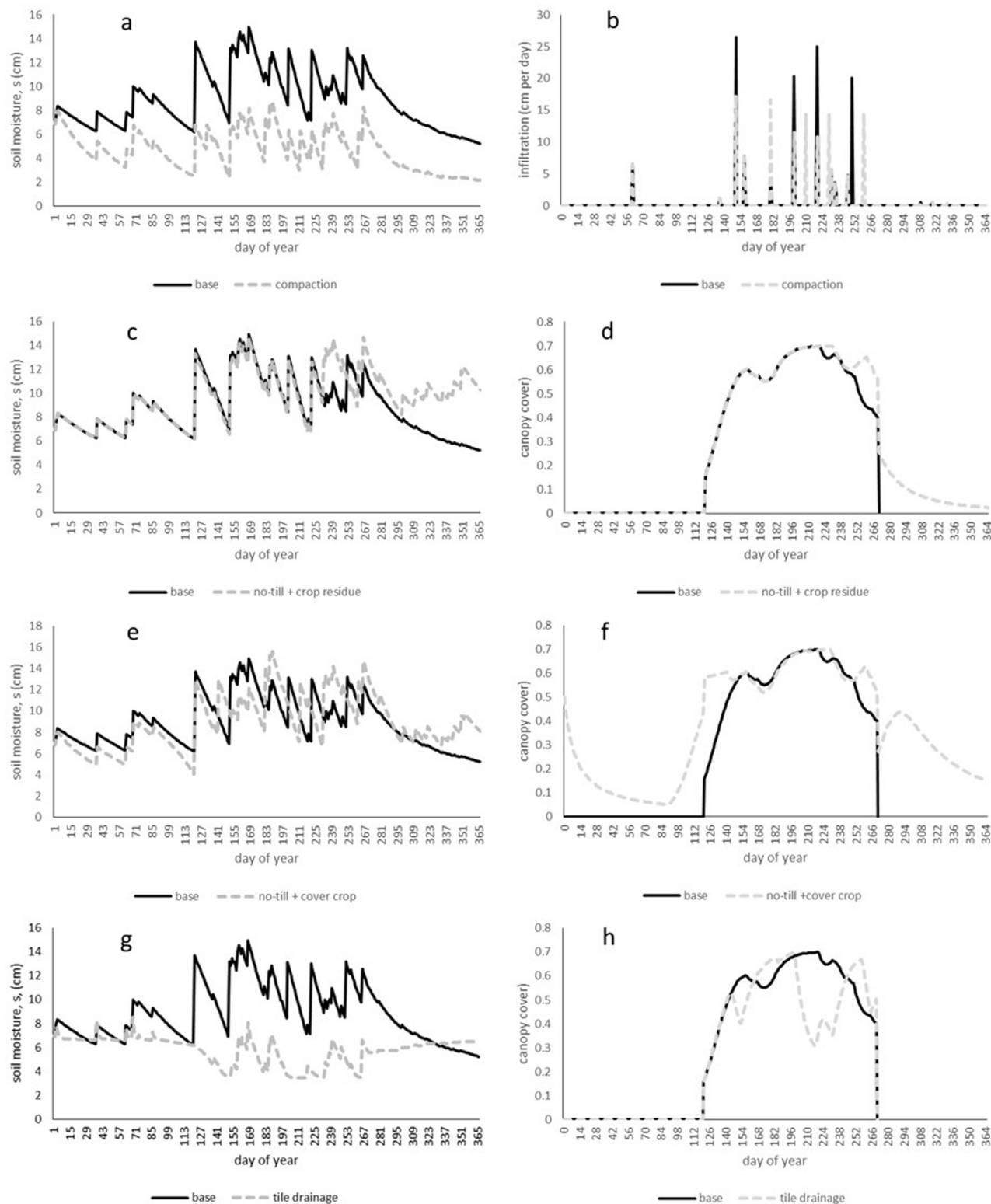


**Figure 12.** Results of the crop management test, illustrating changes in dynamics of soil moisture and infiltration rates from the base case (conventional tillage) due to compaction (panels a and b), and soil moisture and canopy cover under no-till with 50% residual crop biomass (panels c and d), no till with cover cropping (panels e and f), and tile drainage (without irrigation; panels g and h).

profit. Overcoming compaction issues and maintaining adequate pore space for soil water infiltration and storage capacity requires fewer disturbances (such as no-tillage cultivation practices), cover cropping that increases rooting activity and aids in soil aggregation, or some combination of the two. Despite increasing scientific and anecdotal

managerial evidence regarding the benefits of no-till or cover crop practices in cultivated systems, adoption of such practices remain slow (less than 20% in the United States, [United States Department of Agriculture 2017](https://www.usda.gov)). This may be due to reluctance to change tillage practices due to high investment costs for equipment (in the case of no-

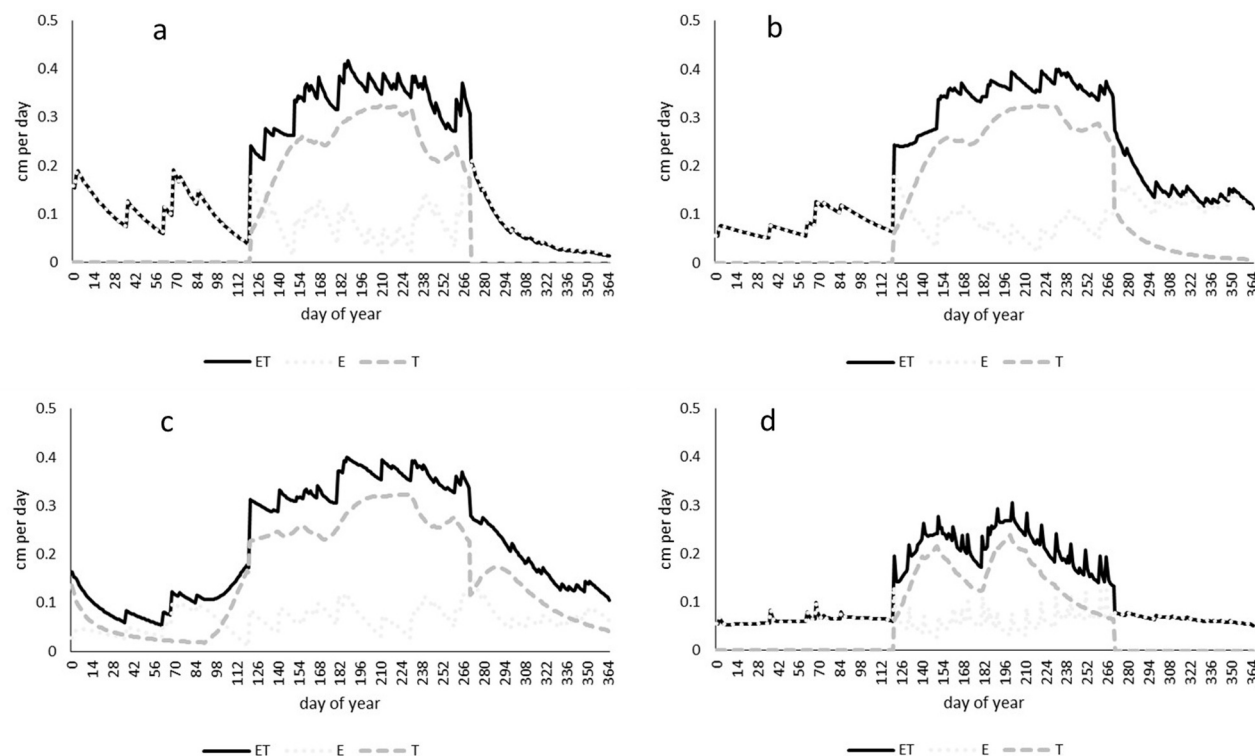


**Figure 13.** Resulting evapotranspiration dynamics from varying crop and soil management parameters accounting for compaction (panel a), no-till with residue management (panel b), no-till with cover cropping (panel c), and tile drainage (panel d); T=transpiration, E=evaporation, and ET=evapotranspiration (T+E).

tillage adoption) or concern that residual soil moisture at the beginning of the cash crop growing season will be lower than optimal due to increase ET induced during the off season (in the case of cover crop adoption). In either case, the model results showed that no-till with residue management or no-till with cover cropping both significantly increased yield and profitability (with cover cropping being the most profitable and 60% greater than no-till with residue management only). In terms of soil moisture, both strategies increased mean soil moisture levels, but only the no-till with residue management was significantly greater than the base case. For agricultural soils similar to those used to parameterize the model for testing, results here show that the benefits in yield and profitability could far outweigh any trade-offs in soil moisture dynamics. Lastly, tile drainage, which is increasingly used in agroecosystems prone to water table rises, in or near wetlands, or other low lying areas, did significantly reduce soil moisture (as well as ET dynamics and plant biomass), but did lead to significant increases in profitability. This provides some economic justification as to why many regions that have experienced recent rapid growth in drain tile installations, including in the grain belt of the United States, despite potential water runoff and quality issues that may arise.

Like traditional ecohydrologic models, the rooting dynamics of various plant or crop types (e.g., shallow vs deep, tap vs fibrous) and the effect that various rooting strategies have on soil aggregation dynamics was not well parameterized and remains an area for future model improvement, especially given the important role that soil aggregation has in regulating soil moisture dynamics (along with inherent soil porosity and depth). Unlike ecohydrologic models, however, we include the transition from canopy cover to soil cover, which facilitated reincorporation of nutrients into the soil column as organic matter is turned over. This provides a clear link to expand the model boundary to include soil microbiology dynamics (i.e., the soil food-web), which would provide a means to scientifically evaluate the physical, chemical, and biological trade-offs that exist in managing the soil processes and function given the variety of goals and constraints of various agroecosystem structures. Although the model data presented here represented

one year at four locations, the model can be simulated for longer time horizons. Preliminary analyses of the long-term (10 year) evolution in soil moisture and other state variables using alternative precipitation and climate parameters indicate the resulting behavior patterns to be robust, however, when feedbacks between management strategies were included, novel behavior patterns in soil moisture, canopy cover, and nutrient dynamics emerge (results not reported here; refining this analysis is the focus of future work described below).

Modeling complex, coupled natural-human systems, including agroecosystems, remains an important inter- and transdisciplinary research area that requires additional effort and attention given the nature of 21st century problems related to agricultural production. Future extensions of this model will require expansion of the model boundaries to include additional irrigation, fertilization, and crop management decision making factors. These may include how producers respond to market or policy signals regarding production decisions (e.g., crop type, planting and harvest dates, environmental penalties due to nutrient leakage, etc.). Even more interesting will be to expand the endogenous decision making factors to examine how those feedbacks may alter optimal input strategies. For example, regions undergoing extensification may see fertilization rates increase above the optimal fertilizer rates to compensate for the lower soil quality soils of newly planted lands that are less suitable for crop production (Alexander et al., 2015, Carpenter et al., 1998, Matson et al., 1997, Tilman et al., 2002, Turner et al., 2018a; Turner et al., 2018b). Similarly, irrigation strategies may be altered from the optimal irrigation rates due to the nature and distribution of water rights. If producers' water rights for allocations will be reduced or removed due to lower water use (potentially stemming from increased production efficiency), then the observed irrigation strategy will likely be higher than the optimal strategy, leading to greater water use and reduced profitability per unit output. On the other hand, where water rights are less clearly defined, producers may opportunistically seek to increase water use as a competitive strategy to out produce competitors or secure a claim to the right based on historical use. A fuller examination of these decision-

making tradeoffs is needed, which will be explored in future applications of the model presented here and described in a companion paper.

## 5. Conclusion

Effective agricultural systems management requires the knowledge and ability to examine and understand, evaluate, and then manage the complex, dynamic (often non-linear) trade-offs that exist at the structural-level of agroecosystems, including soil systems. The soil system dynamics model presented here demonstrated the complex, feedback driven relationships that lie at the center of many soil and resource management problems relevant to agroecosystem management today, namely, the soil moisture-nutrient-plant canopy feedbacks that give rise to the non-linear characteristics of soil moisture and nutrient evolution and crop performance outcomes. Mathematical modeling of such features in agricultural systems remains an area of much needed development if we are to improve our understanding of and ability to manage complex resource management problems (e.g., irrigation, fertilization, soil salinity, soil erosion and/or compaction, etc.) that continue to plague agroecosystems around the world. An important feedback process not explicitly included in the model here is the problem of managerial feedback that captures how managers typically respond to agroecosystem challenges (e.g., over-irrigation or over-fertilization; reluctance to adopt no-till or cover crop practices). In such problems,

modeling efforts require a broader, interdisciplinary perspective beyond the soil system dynamics that include the psychological factors that lead to specific managerial decisions. Modeling efforts that combine those relationships described here with the human dimensions that drive decision-making will help provide a more comprehensive, accurate representation of real-world problems and provide a more solid foundation for evaluating the effectiveness of proposed agricultural policies and strategies aimed at addressing pressing agricultural resource management problems.

## Declaration of Competing Interests

The authors declare that they have no known competing financial interests or personal relationships that could have appeared to influence the work reported in this paper.

## Acknowledgments

This work was partially supported by United States Department of Agriculture's Higher Education Challenge Grant No. 2018-70003-27664 and the National Science Foundation's Center for Research Excellence in Science and Technology (CREST) Award Number 1914745.

## Appendix A

Table A1.

Table A1

Summary of key parameter symbols used throughout the text, including description of the parameter, its value (if a constant) and units, and scientific source from which it was replicated (if applicable).

| List of symbols        | Description  | Value               | Units                  | Source Model or Reference Material  |
|------------------------|--|---------------------|------------------------|---|
| <i>a</i>               | scaling parameter  | -                   | dmnl                   |   |
| B                      | crop biomass   | -                   | kg/m <sup>2</sup>      | (Pelak et al., 2017)  |
| <i>b<sub>e</sub></i>   | the power law exponent   | -                   | dmnl                   | (Pelak and Porporato, 2019)   |
| <i>b<sub>c</sub></i>   | the parameter value at OM equal to 0   | 0.9                 | dmnl                   | (Pelak and Porporato, 2019)   |
| <i>C</i>               | crop canopy cover, the percentage of soil surface covered                                  | -                   | dmnl                   | (Pelak et al., 2017)  |
| CEC                    | Cation Exchange Capacity   | -                   | mmol/gram              | (Mau and Porporato, 2015)   |
| Clc                    | the fraction of canopy becoming surface material   | -                   | dmnl                   |   |
| Clt                    | time to litter fall  | 30                  | day                    |   |
| Cs                     | surface tension of water   | 0.072               | Newton/m               |   |
| Ctt                    | plant litter turnover time   | 90                  | day                    |   |
| D                      | natural deposition rate (assumed constant)   | $15 \times 10^{-6}$ | kg/m <sup>2</sup> /day | (Pelak et al., 2017)  |
| <i>d</i>               | an empirically derived parameter value for the exponential term for saturated conductivity | 13                  | dmnl                   | (Brooks and Corey, 1964, Rodriguez-Iturbe and Porporato, 2004)  |
| <i>dr</i>              | change in radii  | -                   | μm                     | (Pelak and Porporato, 2019)   |
| E                      | evaporation rate   | -                   | cm/day                 | (Laio et al., 2001a, Laio et al., 2001b, Porporato et al., 2015, Porporato et al., 2001, Rodriguez-Iturbe et al., 2001)                     |
| <i>E<sub>b</sub></i>   | baseline evaporation coefficient   | 1.1                 | dmnl                   |   |
| ESP                    | Exchangeable Sodium Percentage   | -                   | dmnl                   | (Mau and Porporato, 2015)   |
| ESR                    | Exchangeable Sodium Ratio  | -                   | mmol/L                 | (Mau and Porporato, 2015)   |
| ET                     | Coupled water losses from evaporation and transpiration                                    | -                   | cm/day                 | (Laio et al., 2001a, Laio et al., 2001b, Porporato et al., 2015, Porporato et al., 2001, Rodriguez-Iturbe et al., 2001)                     |
| ET <sub>0</sub>        | potential evapotranspiration   | -                   | cm/day                 | (Hargreaves, 1975, Hargreaves and Allen, 2003)  |
| ET <sub>lsw</sub>      | water stress coefficient due to limited soil water availability                            | -                   | cm/day                 | (Porporato et al., 2001), Porporato et al 2005, (Laio et al., 2001a, Laio et al., 2001b, Pelak et al., 2017, Rodriguez-Iturbe et al., 2001) |
| E <sub>tw</sub>        | reduced evapotranspiration rate under wilting conditions                                   | -                   | cm/day                 | (Porporato et al., 2001), Porporato et al 2005, (Laio et al., 2001a, Laio et al., 2001b, Pelak et al., 2017, Rodriguez-Iturbe et al., 2001) |
| <i>E<sub>xNa</sub></i> | fraction of sodium in the exchange complex   | -                   | dmnl                   | (Mau and Porporato, 2015)   |
| <i>f</i>               | pore size distribution   | -                   | μm                     | (Pelak and Porporato, 2019)   |
| F                      | fertilization rate at time <i>t</i> of fertilizer application                              | -                   | kg/m <sup>2</sup> /day | (Pelak et al., 2017)  |
| f(η)                   | limitation of nitrogen uptake beyond the critical threshold                                | 0.054               | kg/m <sup>2</sup> /day | (Pelak et al., 2017)  |
| <i>G</i>               | canopy growth rate   | -                   | 1/day                  | (Pelak et al., 2017)  |
| <i>G<sub>e</sub></i>   | Empirically derived value following the Hagen-Poiseuille equation for porous flow          | 1/8                 | dmnl                   | (Brutsaert, 2005, Pelak and Porporato, 2019)  |
| <i>H</i>               | Harvest  | -                   | kg/m <sup>2</sup> /day | (Pelak et al., 2017)  |
| <i>h<sub>i</sub></i>   | harvest index  | 0.5                 | dmnl                   | (Pelak et al., 2017)  |

(continued on next page)

Table A1 (continued)

| List of symbols | Description   | Value                | Units                             | Source Model or Reference Material  |
|-----------------|---|----------------------|-----------------------------------|---|
| $H_d$           | day of harvest  | 270                  | day                               | (Pelak et al., 2017)  |
| $H_v$           | percentage of biomass removed   | 1                    | dmnl                              | (Porporato et al., 2015, Vico and Porporato, 2011a, Vico and Porporato, 2011b)  |
| $I$             | irrigation applications   | -                    | cm/day                            | (Brooks and Corey, 1964, Rodriguez-Iturbe and Porporato, 2004)  |
| $K$             | hydraulic conductivity  | -                    | m/day                             | (Pelak and Porporato, 2019)   |
| $k_b$           | the rate of soil particle settling  | 0.001                | dmnl                              | (Allen et al., 1998)  |
| $K_{cb}$        | basal crop coefficient  | 1.03                 | dmnl                              | (Mau and Porporato, 2015)   |
| $K_g$           | Gapon selectivity coefficient   | $0.0147^{-1/2}$      | mmol/L                            | (Pelak et al., 2017)  |
| $K_r(S)$        | evaporation reduction coefficient   | -                    | dmnl                              | (Brooks and Corey, 1964, Rodriguez-Iturbe and Porporato, 2004)  |
| $K_{sat}$       | saturated hydraulic conductivity  | -                    | m/day                             | (Pelak et al., 2017)  |
| $L$             | leakage term used in N balance equation   | -                    | kg/m/day                          | (Vico and Porporato, 2011a, Vico and Porporato, 2011b)  |
| $li$            | irrigation intervention threshold expressed as a soil moisture percentage of field capacity     | -                    | dmnl                              | (Vico and Porporato, 2011a, Vico and Porporato, 2011b)  |
| $lt$            | target soil moisture level expressed as a soil moisture percentage of field capacity            | -                    | dmnl                              | (Vico and Porporato, 2011a, Vico and Porporato, 2011b)  |
| $LT$            | litter turnover   | -                    | 1/day                             | (Pelak and Porporato, 2019)   |
| $m$             | source-sink term (gain or loss of pores at given radius, $r$ )                                  | -                    | $\mu\text{m}/\text{day}$          | (Pelak et al., 2017)  |
| $M$             | metabolic and senescence rate   | -                    | 1/day                             | (Mau and Porporato, 2015)   |
| $M$             | mass of dry soil  | $2.41e+006$          | $\text{kg}/\text{m}^3$            | (Porporato et al., 2005, Porporato et al 2005, (Laio et al., 2001a, Laio et al., 2001b, Pelak et al., 2017, Rodriguez-Iturbe et al., 2001)  |
| $n$             | soil porosity   | 0.43                 | dmnl                              | (Pelak et al., 2017)  |
| $N_c$           | total mineral nitrogen level per unit area soil   | -                    | $\text{kg}/\text{m}^2$            | (Pelak and Porporato, 2019)   |
| OM (SOM)        | soil organic matter   | -                    | $\text{kg}/\text{m}^3$            | (Pelak and Porporato, 2019)   |
| $P$             | price per unit of crop  | 0.15                 | $"/\text{kg}$                     | (Porporato et al., 2001), Porporato et al 2005, (Laio et al., 2001a, Laio et al., 2001b, Pelak et al., 2017, Rodriguez-Iturbe et al., 2001) |
| $Q(S(t))$       | represents the coupled losses from runoff and percolation below the rooting zone $Z_r$ ,        | -                    | cm/day                            | (Laio et al., 2001a, Laio et al., 2001b, Porporato et al., 2015, Porporato et al., 2001, Rodriguez-Iturbe et al., 2001)                     |
| $q_s$           | salt dissolved in water in the soil column  | -                    | mmol/L                            | (Mau and Porporato, 2015)   |
| $r$             | soil pore radius  | -                    | $\mu\text{m}$                     | (Pelak and Porporato, 2019)   |
| $R(t)$          | inflow of rainfall over time  | -                    | cm/day                            | (Pelak and Porporato, 2019)   |
| $r_b$           | the ratio of the parameter value in an untilled state to the base value                         | 0.9                  | dmnl                              | (Pelak and Porporato, 2019)   |
| $r_g$           | represents a scalar of canopy cover growth per unit of nitrogen utilization                     | 560                  | $\text{m}^2/\text{kg}$            | (Pelak et al., 2017)  |
| $r_m$           | the metabolic constant used in plant senescence   | 0.2                  | 1/day                             | (Pelak et al., 2017)  |
| $Rm(t)$         | maximum effective pore radius   | -                    | $\mu\text{m}$                     | (Pelak and Porporato, 2019)   |
| $S$             | Soil moisture expressed as percentage of field capacity   | -                    | dmnl                              | (Porporato et al., 2001), Porporato et al 2005, (Laio et al., 2001a, Laio et al., 2001b, Pelak et al., 2017, Rodriguez-Iturbe et al., 2001) |
| $S^*$           | soil moisture value below which plants become stressed and begin stomatal closure               | 0.46                 | dmnl                              | (Porporato et al., 2001), Porporato et al 2005, (Laio et al., 2001a, Laio et al., 2001b, Pelak et al., 2017, Rodriguez-Iturbe et al., 2001) |
| $SAR$           | Sodium absorption ratio   | -                    | mmol/L                            | (Mau and Porporato, 2015)   |
| $S_{fc}$        | Full soil moisture saturation   | -                    | cm                                | (Porporato et al., 2001), Porporato et al 2005, (Laio et al., 2001a, Laio et al., 2001b, Pelak et al., 2017, Rodriguez-Iturbe et al., 2001) |
| $S_h$           | the soil moisture value crossing the plant hygroscopic point beyond which moisture losses cease | 0.14                 | dmnl                              | (Porporato et al., 2001), Porporato et al 2005, (Laio et al., 2001a, Laio et al., 2001b, Pelak et al., 2017, Rodriguez-Iturbe et al., 2001) |
| $S_w$           | soil moisture value inducing plant wilting point  | 0.18                 | dmnl                              | (Porporato et al., 2001), Porporato et al 2005, (Laio et al., 2001a, Laio et al., 2001b, Pelak et al., 2017, Rodriguez-Iturbe et al., 2001) |
| $T$             | transpiration   | -                    | cm/day                            | (Pelak et al., 2017)  |
| $t_{sen}$       | estimated time of senescence  | 275                  | day                               | (Pelak et al., 2017)  |
| $ttd$           | time since tillage in days  | -                    | day                               | (Pelak and Porporato, 2019)   |
| $U$             | nitrogen uptake by plant  | -                    | $\text{kg}/\text{m}^2/\text{day}$ | (Pelak et al., 2017)  |
| $v$             | soil drift term for shrinking pore radii  | -                    | $\mu\text{m}$                     | (Pelak and Porporato, 2019)   |
| $V$             | the dissolved salt concentration  | -                    | mmol/L                            | (Mau and Porporato, 2015)   |
| $V_i$           | salt concentration in irrigation water  | 1                    | mmol/L                            | (Mau and Porporato, 2015)   |
| $w^*$           | volumetric water content.   | -                    | $\text{L}/\text{m}^2$             | (Mau and Porporato, 2015)   |
| $x$             | cations in the exchange complex   | -                    | mmol/gram                         | (Mau and Porporato, 2015)   |
| $Y$             | yield   | -                    | $\text{kg}/\text{m}^2$            | (Pelak et al., 2017)  |
| $Z_r$           | soil depth  | 90                   | cm                                | (Porporato et al., 2001), Porporato et al 2005, (Laio et al., 2001a, Laio et al., 2001b, Rodriguez-Iturbe et al., 2001)                     |
| $\gamma$        | slope of the senescence curve post-tsen   | 0.005                | 1/day                             | (Pelak et al., 2017)  |
| $\gamma_b$      | management factor used in the b term  | -                    | dmnl                              | (Pelak and Porporato, 2019)   |
| $\gamma_w$      | specific weight of water  | 0.001                | $\text{kg}/\text{cm}^3$           | (Pelak and Porporato, 2019)   |
| $\eta$          | nitrogen content of soil moisture   | 1                    | $\text{kg}/\text{m}^2$            | (Pelak et al., 2017)  |
| $\eta_c$        | critical threshold of nitrogen beyond which plant uptake does not occur                         | 1                    | $\text{kg}/\text{m}^3/\text{day}$ | (Pelak et al., 2017)  |
| $\Theta$        | step function that causes crop canopy senescence to begin                                       | -                    | 1/day                             | (Pelak et al., 2017)  |
| $\mu$           | dynamic viscosity of water  | $8.9 \times 10^{-4}$ | Pa                                | (Pelak and Porporato, 2019)   |
| $\sigma_b$      | slope of the b-OM relationship  | -0.001               | dmnl                              | (Pelak and Porporato, 2019)   |
| $\psi_s$        | matric potential  | -                    | MPa                               | (Pelak and Porporato, 2019)   |

## References

Abd, E.M.H., Ali, E.A., 2013. Effect of irrigation systems, amounts of irrigation water and mulching on corn yield, water use efficiency and net profit. *Agricultural Water Management* 120, 64–71.

Adhikari, K., Hartemink, A.E., 2016. Linking soils to ecosystem services—A global review. *Geoderma* 262, 101–111.

Alexander, P., Rounsevell, M.D.A., Dislich, C., Dodson, J.R., 2015. Drivers for global agricultural land use change: the nexus of diet, population, yield, and bioenergy. *Global Environmental Change* 35, 138–147.

Ali, M.H., Hoque, M.R., Hassan, A.A., Khair, A., 2007. Effects of deficit irrigation on yield, water productivity, and economic returns of wheat. *Agricultural Water Management* 92, 151–161.

Allen, R.G., Pereira, L.S., Raes, D., Smith, M. 1998. FAO Irrigation and Drainage Paper 56: Crop Evapotranspiration (Guidelines for Computing Crop Water Requirements).

Bennett, J.M., Mutti, L.S.M., Rao, P.S.C., Jones, J.W., 1989. Interactive effects of nitrogen and water stresses on biomass accumulation, nitrogen uptake, and seed yield of maize. *Field Crop Research* 19, 297–311.

Bernstein, L., 1975. Effects of salinity and sodicity on plant growth. *Annual Review of Phytopathology* 13 (1), 295–312.

Brady, N.C., Weil, R.R., 1996. The nature and properties of soils, 11th edition. Prentice-Hall, Upper Saddle River, NJ.

Branson, F.A., Miller, R.F., McQueen, I.S., 1970. Plant communities and associated soil and water factors on shale-derived soils in Northeastern Montana. *Ecology* 51 (3), 391–407.

Branson, F.A., Miller, R.F., McQueen, I.S., 1976. Moisture relationships in twelve northern desert shrub communities near Grand Junction, Colorado. *Ecology* 57 (6), 1104–1124.

Brooks, R., Corey, T., 1964. Hydraulic properties of porous media. *Hydrology Papers*. Colorado State University.

Brutsaert, W., 2005. Hydrology: An introduction.

Carpenter, S.R., Caraco, N.F., Correll, D.L., Howarth, R.W., Sharpley, A.N., Smith, V.H., 1998. Nonpoint pollution of surface waters with phosphorus and nitrogen. *Ecological applications* 8 (3), 559–568.

Clapp, R.B., Hornberger, G.N., 1978. Empirical equations for some soil hydraulic properties. *Water Resources Research* 14 (8), 601–604.

Daly, E., Porporato, A., 2006. Impact of hydroclimate fluctuations on the soil water balance. *Water Resources Research* 42 (6), W06401.

Daubenmire, R., 1968. Soil moisture in relation to vegetation distribution in the mountains of northern Idaho. *Ecology* 49 (3), 431–438.

De Michele, C., Vezzoli, R., Pavlopoulos, H., Scholes, R.J., 2008. A minimal model of soil water-vegetation interactions forced by stochastic rainfall in water-limited ecosystems. *Ecological Modelling* 212, 397–407.

Denholm, I., 1998. Challenges with managing insecticide resistance in agricultural pests, exemplified by the whitefly *Bemisia tabaci*. *Philosophical Transactions of the Royal Society B: Biological Sciences* 353 (1376), 1757.

Droogers, P., Kite, G., Murray-Rust, H., 2000. Use of simulation models to evaluate irrigation performance including water productivity, risk, and system analyses. *Irrigation Science* 19 (3), 139–145.

Duncan, R.A., Bethune, M.G., Thayalakumaran, T., Christen, E.W., McMahon, T.A., 2008. Management of salt mobilization in the irrigated landscape – A review of selected irrigation regions. *Journal of Hydrology* 351, 238–252.

Falkenmark, M., Rockstrom, J., 2006. The New Blue and Green Water Paradigm: Breaking New Ground for Water Resources Planning and Management. *Journal of Water Resources Planning and Management* May/June 129–132.

Fernald, A.G., Yeliz Cevik, S., Ochoa, C.G., Tidwell, V.C., Phillip King, J., Guldan, S.J., 2010. River hydrograph retransmission function of irrigated valley surface water-groundwater interactions. *Journal of Irrigation and Drainage Engineering* 136 (12), 823–835.

Fernald, A., Tidwell, V., Rivera, J., Rodriguez, S., Guldan, S., Steele, C., Ochoa, C., Hurd, B., Ortiz, M., Boykin, K., Cibils, A., 2012. Modeling sustainability of water, environment, livelihood, and culture in traditional irrigation communities and their linked watersheds. *Sustainability* 4 (11), 2998–3022.

Ford, A., Flynn, H., 2005(Winter 2005). Statistical screening of system dynamics models. *System Dynamics Review* 21 (4), 273–303.

Gates, T.K., Burkhalter, J.P., Labadie, J.W., Valliant, J.C., Broner, I., 2002. Monitoring and modeling flow and salt transport in a salinity-threatened irrigated valley. *Journal of Irrigation and Drainage Engineering* 128 (2), 87–99.

Gunda, T., Turner, B.L., Tidwell, V.C., 2018. The influential role of sociocultural feedbacks on community-managed irrigation system behaviors during times of water stress. *Water Resources Research* 54 (4), 2697–2714.

Hargreaves, G.H., 1975. Moisture availability and crop production. *Trans. ASAE* 18, 980–984.

Hargreaves, G.H., Allen, R.G., 2003. History and evaluation of Hargreaves evapotranspiration equation. *J. Irrig. Drain. Eng. ASCE* 129, 53–63.

Harrington, G.N., 1991. Effects of soil moisture on shrub seedling survival in a semi-arid grassland. *Ecology* 72 (3), 1138–1149.

Horrigan, L., Lawrence, R.S., Walker, P., 2002. How sustainable agriculture can address the environmental and human health harms of industrial agriculture. *Environmental Health Perspectives* 110, 445–456.

Hsiao, T.C., Heng, L., Steduto, P., Rojas-Lara, B., Raes, D., Fereres, E., 2009. Aquacrop – the FAO crop model to simulate yield response to water: III. Pattermaterization and testing for maize. *Agronomy Journal* 101, 448–459.

Hurni, H., Giger, M., Liniger, H., Studer, R.M., Messerli, P., Portner, B., Schwilch, G., Wolfgramm, B., Breu, T., 2015. Soils, agriculture and food security: the interplay between ecosystem functions and human well-being. *Current Opinions in Environmental Sustainability* 15, 25–34.

International Fertilizer Association. 2019. Accessed <https://www.ifastat.org/>, October 30, 2019.

Konikow, L.F., 2013. Groundwater depletion in the United States (1900–2008).

Konikow, L.F., Kendy, E., 2005. Groundwater depletion: A global problem. *Hydrogeology Journal* 13 (1), 317–320.

Konikow, L.F., Person, M., 1985. Assessment of long-term salinity changes in an irrigated stream-aquifer system. *Water Resources Research* 21 (11), 1611–1624.

Kranthi, K.R., Jadhav, D.R., Kranthi, S., Wanjari, R.R., Ali, S.S., Russell, D.A., 2002. Insecticide resistance in five major insect pests of cotton in India. *Crop Protection* 21 (6), 449–460.

Kumar, R., Jat, M.K., Shankar, V., 2013. Evaluation of modeling of water ecohydrologic dynamics in soil-root system. *Ecological Modelling* 269, 51–60.

Laio, F., Porporato, A., Ridolfi, L., Rodriguez-Iturbe, I., 2001a. Plants in water-controlled ecosystems: active role in hydrologic processes and response to water stress II. Probabilistic soil moisture dynamics. *Advances in Water Resources* 24, 707–723.

Laio, F., Porporato, A., Ridolfi, L., Rodriguez-Iturbe, I., 2001b. Plants in water controlled ecosystems: active role in hydrologic processes and response to water stress-IV. Discussion of real cases. *Advances in Water Resources* 24 (7), 707–723.

Larcher, W., 1995. Physiological plant ecology, 3rd edition. Springer, Berlin.

Manzoni, S., Porporato, A., 2009. Soil carbon and nitrogen mineralization theory and models across scales. *Soil Biology and Biochemistry* 41, 1355–1379.

Matson, P.A., Parton, W.J., Power, A.G., Swift, M.J., 1997. Agricultural intensification and ecosystem properties. *Science* 277 (5325), 504–509.

Mau, Y., Porporato, A., 2015. A dynamical system approach to soil salinity and sodicity. *Advances in Water Resources* 83, 68–76.

Mendelsohn, R., Basist, A., Dinar, A., Kurukulasuriya, P., Williams, C., 2007. What explains agricultural performance: climate normal or climate variance? *Climate Change* 81 (1), 85–99.

Menendez, H.M., Wuellner, M.R., Turner, B.L., Gates, R.N., Dunn, B.H., Tedeschi, L.O., 2019. A spatial landscape scale approach for estimating erosion, water quantity, and quality in response to South Dakota grassland conversion. *Natural Resource Modeling*. <https://doi.org/10.1111/nrm.12243>.

Molden, D. (Ed.), 2007. Water for food, water for life. Earthscan, London, UK.

Montgomery, D.R., 2007. Soil erosion and agricultural sustainability. *Proceedings of the National Academy of Sciences* 104 (33), 13268–13272.

Motha, R.P., Baier, W., 2005. Impacts of present and future climate change and climate variability on agriculture in the temperate regions: North America. *Climate Change* 70 (1–2), 137–164.

Mualem, Y., Dagan, G., 1978. Hydraulic conductivity of soils: unified approach to the statistical models 1. *Soil Sci Soc Am J* 42 (3), 392–395.

Nearing, M.A., Xie, Y., Liu, B., Ye, Y., 2017. Natural and anthropogenic rates of soil erosion. *International Soil and Water Conservation Research* 5 (2), 77–84.

Nearing, M.A., Jetten, V., Baffaut, C., Cerdan, O., Couturier, A., Hernandez, M., Le Bissonnais, Y., Nichols, M.H., Nunes, J.P., Renschler, C.S., Souchère, V., 2005. Modeling response of soil erosion and runoff to changes in precipitation and cover. *Catena* 61 (2–3), 131–154.

Newman, E.I., 1967. Response to *Aira praecox* to weather conditions. I. Response to drought in spring. *Journal of Ecology* 55 (2), 539–556.

Nilsen, E.R., Orcutt, D.M., 1998. Physiology of plant under stress: abiotic factors. Wiley, New York.

Niu, G., Cabrera, R.I., 2010. Growth and Physiological Responses of Landscape Plants to Saline Water Irrigation: A Review. *HortScience* 45, 1605–1609.

Oliva, R., 1995. A Vensim® Module to Calculate Summary Statistics for Historical Fit. System Dynamics Group, MIT, Memo D-4584.

Pan, F., Nieswiadomy, M., Qian, S., 2015. Application of a soil moisture diagnostic equation for estimating root-zone soil moisture in arid and semi-arid regions. *Journal of Hydrology* 524, 296–310.

Pelak, N., Revelli, R., Porporato, A., 2017. A dynamical systems framework for crop models: Toward optimal fertilization and irrigation strategies under climatic variability. *Ecological Modelling* 365, 80–92.

Pelak, N., Porporato, A., 2019. Dynamic evolution of the soil pore size distribution and its connection to soil management and biogeochemical processes. *Advances in Water Resources* 131, 103384.

Pimentel, D., Acquay, H., Biltonen, M., Rice, P., Silva, M., Nelson, J., Lipner, V., Giordano, S., Horowitz, A., D'amore, M., 1992. Environmental and economic costs of pesticide use. *BioScience* 42 (10), 750–760.

Porporato, A., D'Odorico, P., Laio, F., Ridolfi, L., Rodriguez-Iturbe, I., 2002. Ecohydrology of water-controlled ecosystems. *Advances in Water Resources* 25, 1335–1348.

Porporato, A., Feng, X., Manzoni, S., Mau, Y., Parolari, A.J., Vico, G., 2015. Ecohydrological modeling in agroecosystems: Examples and Challenges. *Water Resources Research* 51, 5081–5099.

Porporato, A., Laio, F., Ridolfi, L., Rodriguez-Iturbe, I., 2001. Plants in water-controlled ecosystems: active role of hydrologic processes and response to water stress III. Vegetation water stress. *Advances in Water Resources* 24, 725–744.

Power, A.G., 2010. Ecosystem services and agriculture: tradeoffs and synergies. *Phil. Trans. R. Soc. B* 365, 2959–2971.

Qadir, M., Oster, J.D., 2004. Crop and irrigation management strategies for saline-sodic soils and waters aimed at environmentally sustainable agriculture. *Science of the Total Environment* 323, 1–19.

Quiring, S.M., Ford, T.W., Wang, J.K., Khong, A., Harris, E., Lindgren, T., Goldberg, D.W., Li, Z., 2016. The North American Soil Moisture Database Development and Applications. *Bulletin of the American Meteorological Society (BAMS)* 1441–1459.

<https://doi.org/10.1175/BAMS-D-13-00263.1>. August.

Rodriguez-Iturbe, I., D'Odorico, P., Porporato, A., Ridolfi, L., 1999. On the spatial and temporal links between vegetation, climate and soil moisture. *Water Resources Research* 35 (12), 3709–3722.

Rodriguez-Iturbe, I., 2000. Ecohydrology: A hydrologic perspective of climate-soil-vegetation dynamics. *Water Resources Research* 36 (1), 3–9.

Rodriguez-Iturbe, I., Porporato, A., Laio, F., Ridolfi, L., 2001. Plants in water-controlled ecosystems: active role in hydrologic processes and response to water stress I. Scope and general outline. *Advances in Water Resources* 24, 695–705.

Rodriguez-Iturbe, I., Porporato, A., 2004. *Ecohydrology of Water Controlled Ecosystems: Soil Moisture and Plant Dynamics*. Cambridge University Press.

Roush, R., Tabashnik, B.E. (Eds.), 2012. *Pesticide resistance in arthropods*. Springer Science & Business Media.

Sadras, V.O., Angus, J.F., 2006. Benchmarking water-use efficiency of rainfed wheat in dry environments. *Australian Journal of Agricultural Research* 57, 847–856.

Scanlon, B.R., Jolly, I., Sophocleous, M., Zhang, L., 2007. Global impacts of conversions from natural to agricultural ecosystems on water resources: Quantity versus quality. *Water Resources Research* 43 (3).

Seneviratne, S.I., Corti, T., Davin, E.L., Hirschi, M., Jaeger, E.B., Lehner, I., Orlowsky, B., Teuling, A.J., 2010. Investigating soil moisture-climate interactions in a changing climate: A review. *Earth-Science Reviews* 99, 125–161.

Smedema, L.K., Shiati, K., 2002. Irrigation and salinity: a perspective review of the salinity hazards of irrigation development in the arid zone. *Irrigation and Drainage Systems* 16 (2), 161–174.

Stephenson, N.L., 1990. Climatic control of vegetation distribution: the role of the water balance. *American Naturalist* 135 (5), 649–670.

Swift, M.J., Izac, A.M.N., van Noordwijk, M., 2004. Biodiversity and ecosystem services in agricultural landscapes: are we asking the right questions? *Agric. Ecosyst. Environ.* 104, 113–134.

Tedeschi, L., 2005. Assessment of the adequacy of mathematical models. *Agricultural Systems* 89, 225–247.

Texas Water Development Board (2019). Accessed <https://waterdatafortexas.org/groundwater>, October 30, 2019.

Tilman, D., Cassman, K.G., Matson, P.A., Naylor, R., Polasky, S., 2002. Agricultural sustainability and intensive production practices. *Nature* 418 (6898), 671.

Turner, B.L., Tidwell, V., Fernald, A., Rivera, J.A., Rodriguez, S., Guldian, S., Ochoa, C., Hurd, B., Boykin, K., Cibils, A., 2016a. Modeling acequia irrigation systems using system dynamics: model development, evaluation, and sensitivity analyses to investigate effects of socio-economic and biophysical feedbacks. *Sustainability* 8 (10), 1019.

Turner, B.L., Wuellner, M., Nichols, T., Gates, R., Tedeschi, L., Dunn, B., 2016b. Development and evaluation of a system dynamics model for investigating agriculturally driven land transformation in the north central United States. *Natural Resource Modeling* 29 (2), 179–228.

Turner, B.L., Menendez, H.H., Gates, R., Tedeschi, L.O., Atzori, A.S., 2016c. System dynamics modeling for agricultural and natural resource management issues: review of some past cases and forecasting future roles. *Resources* 5 (4), 40. <https://doi.org/10.3390/resources5040040>.

Turner, B.L., Wuellner, M., Nichols, T., Gates, R., Tedeschi, L.O., Dunn, B.H., 2017a. A systems approach to forecast agricultural land transformation and soil environmental risk from economic, policy, and cultural scenarios in the north central United States (2012–2062). *International Journal of Agricultural Sustainability* 15 (2), 102–123.

Turner, B.L., 2017b. Development and evaluation of an ecohydrology soil-moisture model to aid in understanding semi-arid ecosystem dynamics. Presented at the 35th International Conference of the System Dynamics Society, available at <https://www.systemdynamics.org/assets/conferences/2017/proceed/papers/P1073.pdf>.

Turner, B.L., Fuhrer, J., Wuellner, M., Menendez, H.M., Dunn, B.H., Gates, R., 2018a. Scientific case studies in land-use driven soil erosion in the central United States: Why soil potential and risk concepts should be included in the principles of soil health. *International Soil and Water Conservation Research* 6 (1), 63–78.

Turner, B.L., Wuellner, M., Malo, D.D., Herrick, J.E., Dunn, B.H., Gates, R., 2018b. Ecosystem functions in mixed cropland–grassland systems influenced by soil legacies of past crop cultivation decisions. *Ecosphere* 9 (12), e02521.

United States Department of Agriculture. 2014. Farm and Ranch Irrigation Survey 2013, Volume 3, Special Studies, Part 1, AC-12-SS-1, November 2014. Accessed [https://www.nass.usda.gov/Publications/AgCensus/2012/Online\\_Resources/Farm\\_and\\_Ranch\\_Irrigation\\_Survey/](https://www.nass.usda.gov/Publications/AgCensus/2012/Online_Resources/Farm_and_Ranch_Irrigation_Survey/), October 20, 2019.

United States Department of Agriculture 2017. U.S. Census of Agriculture. Accessed <https://www.nass.usda.gov/Publications/AgCensus/2017/index.php>.

Vico, G., Porporato, A., 2011a. From rainfed agriculture to stress-avoidance irrigation: I. A generalized irrigation scheme with stochastic soil moisture. *Advances in Water Resources* 34 (2), 263–271.

Vico, G., Porporato, A., 2011b. From rainfed agriculture to stress-avoidance irrigation: II. Sustainability, crop yield, and profitability. *Advances in Water Resources* 34 (2), 272–281.

Vico, G., Porporato, A., 2013. Probabilistic description of crop development and irrigation water requirements with stochastic rainfall. *Water Resources Research* 49, 1466–1482.

Wang, Q., Li, F., Zhang, E., Li, G., Vance, M., 2012. The effects of irrigation and nitrogen application rates on yield of spring wheat (longfu-920), and water use efficiency and nitrate nitrogen accumulation in soil. *Australian Journal of Crop Science* 6, 662–672.

Wichelns, D., Qadir, M., 2015. Achieving sustainable irrigation require effective management of salts, soils salinity, and shallow groundwater. *Agricultural Water Management* 157, 31–38.

Xia, Y.Q., Shao, M.A., 2008. Soil water carrying capacity for vegetation: A hydrologic and biogeochemical process model solution. *Ecological Modelling* 214, 112–124.